GChron Response to Reviewers Round 2

Comments to the Author:

Dear Travis and colleagues,

Thank you for taking the time to substantially revise your manuscript. I asked two of the original referees to review your revised manuscript. You will see that one of these referees had additional concerns, particularly about eq. 4 and the combination of a transient erosion model with a steady-state flux calculation. I kindly ask you to consider these new reviewer comments in a revised version of the text. The other referee only had a handful of minor, technical corrections that should be easy to incorporate.

Thank you again for the hard work you have put into this manuscript thus far. Pending this second round of revisions, I believe your manuscript will be publishable in Geochronology.

All the best,

Marissa

Hi Marissa,

Thank you again for facilitating this round of reviews. Below, we have addressed all of the concerns and comments from the reviewers, and feel we have properly justified:

1) Our updated approach of utilizing a transient erosion model with a steady-state flux calculation

2) That these moraines are indeed in steady state

3) That Eq. 4 is not in error

4) Our paleomagnetic normalization approach

To the last point, we have included a very detailed description of our approach along with a worked example -- both in the response to the reviewer, as well as in the Supplementary Material for the manuscript, including a helpful flowchart. Finally, we have decided to no longer use Monte Carlo simulations to determine uncertainties, as using traditional algebraic uncertainty propagation achieves the same result in a much simpler and easier to follow fashion. We believe our manuscript is now even stronger than before, and we thank the reviewers for their time and consideration in helping us improve this work.

Best,
Travis and co-authors

Reviewer 1

I have reviewed the revised text of "Calibrating a long-term meteoric 10Be delivery rate into eroding Western US glacial deposits by comparing meteoric and in situ produced 10Be depth profiles". The revised text is far clearer and better organized. However, as I now finally understand the methods employed, I have some new concerns to present.

First, the final term of equation 4 must be dropped. The 10Be that does not sorb in the topsoil layer would normally sorb at depth as infiltration continues and become part of the inventory. Under the steady state assumptions behind equation 4, 10Be delivered to the soil at depth is already counted in the loss to decay term. If the authors believe that 10Be is genuinely lost to ground water and not sorbed to the soil at any depth, the loss to ground water must be in terms of the entire inventory, not merely the surface layer. However, it is hard to imagine loss to groundwater at depth in this context, given the pedogenic carbonate build up in the soil. In principle, there could be a surface runoff term. But you'd need to calculate the proportion of precipitation that exits the system as overland flow, which I imagine is fairly small even in this semiarid context.

The reviewer is right in pointing out that an assumption built into Eq. 4 is that all dissolved ^{10}Be loss takes place at the surface. This is due to the steady state mixed reactor framework used by von Blanckenburg et al. (2012). This assumption becomes apparent as we use a surface $[^{10}Be]_{reac}$ to calculate a surface $[^{10}Be]_{diss}$ via Kd. The reviewer is also right to say that, if fluid is discharged from depth and ^{10}Be is desorbed at depth, $[^{10}Be]_{diss}$ will be lower because $[^{10}Be]_{reac}$ is lower at depth (but it likely won't be zero, see below, nor do we see a large role for radiodecay given the young age of the moraines compared to the ^{10}Be half life of 1.4My). Calculating this loss in terms of the inventory, as the reviewer suggests, would be best. However, this would require knowing the geometry and flux of fluid flow at any given depth, even to beneath the ^{10}Be adsorption depth. This amounts to an impossible task.

The reviewer thus suggests removing the Q/Kd correction wholesale, thereby assuming that 100% of the delivered meteoric ^{10}Be is adsorbed either at the surface or at depth. That assumption also does not hold true for this site, because of the pH (5.5 to 8 at depth) and associated Kd value here. Q/Kd is not sufficiently small compared to the erosion rate (von Blanckenburg et al,. 2012, Fig. A1). We thus cannot exclude the term and must consider retention for this to be a valid study.

In the revised version we thus emphasize that this loss correction represents an "maximum bound". Regardless, we note again that our retention calculations using Eq. 4 indicate that there is not substantial loss due to desorption. In the worst case scenario, with the lowest Kd estimate, the bias is only ~4% and ~9% for Pinedale and Bull Lake, respectively. At an average estimated Kd value (5.5E5 L/kg) for these sites, the bias is only ~1% and ~2%, respectively. We thank the reviewer for encouraging us to present a more explicit perspective of this previously implicit assumption.

Secondly, I don't think it's reasonable to blithely combine a transient erosion model with a steady state flux calculation. The period of highest erosion would have occurred before

steady state was reached, while 10Be in the eroding topsoil was at significantly lower concentrations. The authors are therefore almost certainly overstating loss of 10Be to erosion and therefore overstating deposition. Furthermore, I doubt the 10Be profile in the Pinedale Moraine is anywhere close to steady state, even if erosion were steady (the Bull Lake may be). Depending on erosion rate and erosive depth, the time to steady state can potentially be hundreds of thousands of years (Graly et al., 2010). The authors need to create a transient model of 10Be development in the soil. I know they'd rather not, but there really isn't any way around this.

This comment consists of two parts. Part 2 suggests that the meteoric ^{10}Be is nowhere close to steady state and suggests that the time to steady state can be "hundreds of thousands of years". We strongly disagree with this assessment. We calculate the integration time scale of these erosion rates by dividing the adsorption depth (1/k = 20 and 30 cm for Pinedale and Bull Lake, respectively) by the erosion rate for each moraine and find that the integration time scales are 6 ky and 24 ky for Pinedale and Bull Lake, respectively. It's reasonable to assume that steady state is achieved after ~4-5 integration time scales have passed (Willenbring & von Blanckenburg, 2010), which corresponds to 24-30 ky for Pinedale, and 96-120 ky for Bull Lake. Given that the depositional age is 21-25 ky for Pinedale, and 140 ky for Bull Lake this justifies our consideration that these profiles are indeed in cosmogenic steady state. We have now made this point more apparent in the revised version.

Part 1 of the comment suggests that we should not calculate a meteoric ^{10}Be flux (from Eq.4) using a constant erosion rate while at the same time basing this erosion rate on a transient erosion model. This is a valid statement to make. The reviewer also guesses correctly that we are indeed highly reluctant to design a transient model of meteoric ^{10}Be accumulation, which would require a very substantial set of assumptions that would be close to impossible to constrain. A way around this would be to adopt the framework of Lal and Chen (2005), as Schaller et al. (2009a) did, but for meteoric ^{10}Be, to constrain both age and erosion rate. However, their equations depend on the existence of a mixing zone, which we do not observe for meteoric ^{10}Be in these profiles, so this is not possible. Thus, we maintain that while it is true that the transient erosion model indicates that erosion is fastest after initial deposition, the transient erosion rate modeled by Schaller et al. 2009, that we now use in this study, is not an "end-member rate" in the sense that the moraines were only eroding at 32 and 13 mm/ky for Pinedale and Bull Lake, respectively, during the initial wave of fast erosion, before the moraine evolved to the less flat-topped morphology we observe today. Instead, these rates are integrated over the entire age of the moraine, such that they capture the average of all erosion that has occurred at the moraine crests over these time periods. If we instead used the constant erosion model, we'd certainly be understating the loss of ^{10}Be to erosion! Thus, we feel justified using the transient erosion model, as it gives us the most valid estimate of the true erosion rates for these landforms given what we know about hillslope diffusion. We have added explanatory text to section 3.2 making the reader aware of this potential complication as follows:

> *"This approach integrates this transient behavior over the entire age of each moraines, and thus likely overstates the loss of ^{10}Be to erosion to some degree, however it nonetheless provides the most realistic estimates possible for these moraines as we are otherwise unable to independently constrain their site-specific erosion rates"*

Finally, the paleo-magnetic corrections remain poorly explained. No equations are provided nor is any data presented, save the final corrected numbers. A supplemental table that completely explains this is required.

All information that is needed to calculate the paleomagnetic corrections is in Table 3 (there was previously a typo for the correction factor relative to Holocene for Graly et al. 2011, however -- this was just a drafting error [not used in calculations] and has been fixed) and the references provided (Masarik & Beer 2009; Christl et al. 2010; Steinhilber et al. 2012). Maybe the reviewer is looking for a formula for converting paleomagnetic field strength and solar modulation into ^{10}Be production. We do not use any. We simply linearly transform fluxes for a given integration time into another flux for another integration time, and to do so we use the graphs in Masarik & Beer (2009) and the conversion factors for the Holocene from Steinhilber et al. (2012), Fig. 3B. Please see our response to your line 287 comment below for a more detailed explanation. We added more explicit details of our treatment to the text as follows:

> *As the estimations of flux from Graly et al. (2011) were normalized to reflect a solar modulation of 700 MV, we rescaled the modern Graly-derived $F_{(10Bemet)}$ to the average Holocene solar modulation factor of 280.94 MV used in the flux map of Heikkilä and von Blanckenburg (2015) following the paleomagnetic and solar intensity normalization procedure of Deng et al. (2020). This is carried out by first rescaling production at 700 MV to 500 MV (i.e. the modern solar modulation value of Steinhilber et al., 2012) via Fig. 4B of Masarik & Beer (2009) for a Graly et al. (2011)-specific modern scaling factor of 0.82 (Table 3). Then, to properly normalize for the Holocene, we multiply this modern scaling factor by the reciprocal of the rescaling factor of Heikkilä and von Blanckenburg (2015) (1.23) to arrive at a Holocene-normalized scaling factor of 0.67 and apply this to the Graly et al. (2011) flux estimate (Table 3). We illustrate and further describe the details of this procedure in the Supplementary Material (Fig. S1).*

We have also added a flowchart to the Supplemental Material (Fig. S1) that takes the reader through each step of the calculation, with a worked example, to help illustrate and better describe the treatment. We feel this will be further beneficial to any reader that may want/need to carry out normalizations like these in the future.

To clarify how the moraine accumulation were corrected (integration time scales are 6 ky and 24 ky for Pinedale and Bull Lake, respectively) we have modified the text beginning line 251 as follows:

> *"To further compare the model- and the precipitation-derived Holocene-average $F_{(10Bemet)}$ estimates with those calculated in this study, we must also normalize for geomagnetic and solar intensity variations within the Holocene (for Pinedale,with a 6 ky cosmogenic integration time) and beyond the Holocene (Bull Lake, with a 24 ky cosmogenic integration time). We again linearly rescaled our calculated loss-corrected $F_{(10Bemet)}$ for the and Bull Lake moraines by first integrating the production rate relative to the modern using the Principle Component 1 (PC1) of the ^{10}Be marine core record of Christl et al. (2010), converting PC1 into relative fluxes from 6 ky and 24 ky, respectively, and then normalizing these values to those over the Holocene, propagating the statistical uncertainties. These time intervals represent the calculated residence/integration times of the soil profiles from the surface to the e-folding adsorption depth of $^{10}Be_{met}$ (20 and 30 cm for the Pinedale and Bull Lake moraines, respectively). This approach accounts for the*

cumulative effects of transient erosion and leaching by weighting geomagnetic intensity variations on $F_{(10Bemet)}$ towards the present."

Some line-by-line comments:

116: No justification is given here for why the industrial run is a reasonable upper bound on the paleo 10Be fallout. Nor is it explained why industrial processes would make 10Be flux nearly a factor of 2 higher in this location.

Heikkila and von Blanckenburg (2015) explicitly describe how to determine uncertainty on their estimated fluxes -- it is the difference between the Modern and Pre-Industrial model runs, which is what we report as the uncertainty. Here is their explanation from their dataset:

> *"Modern ("Industrial") Model: Direct output from ECHAM5-HAM modern atmosphere and aerosol loading was used from a 30 year run simulating the modern atmosphere characterised by industrial aerosol and greenhouse gas loading (Heikkilä et al., 2013a, Heikkilä and Smith, 2013c).*
>
> *"Pre-Industrial" model: The model is ECHAM5-HAM, run with preindustrial aerosol and greenhouse gas concentrations (Heikkilä et al., 2013b). The global flux of the pre-industrial model was adjusted to represent the same cosmic ray production rate as in the modern model.*
>
> *Average Model: The Modern and the Pre-Industrial model was combined by averaging. (Dark green Sheet).* ***The difference between both can be used as a rough uncertainty estimate*** *(light green sheet). The difference results from climate-dependent shifts in delivery of 10Be, but not on changes in its production."*

We have added this information to the text as follows:

> *"We use the pre-industrial modeled $F_{(10Bemet)}$ in our comparisons, as it is a more appropriate estimate for landforms of these ages. To place an upper bound uncertainty on this estimate, which is otherwise hard to quantify, we utilize the difference between the industrial and pre-industrial predicted $F_{(10Bemet)}$ ($+0.99 \times 10^6$ atoms cm^{-2} y^{-1}). This difference is solely a result of climate-dependent shifts in the delivery of $^{10}Be_{met}$ and shifts resulting from large industrial aerosol loading in modern times and does not reflect changes in atmospheric production (Heikkilä and von Blanckenburg, 2015)."*

163-165: I find this statement deeply unsettling. Of course, you know where the mass loss occurred. That is the whole point of conservative tracer approaches. You know exactly, down to 10 cm scale, which elements leached out of the profile and in which abundances.

We are not entirely sure what point the reviewer is making here, nor what he means with "conservative tracer approaches", or how we would exactly know the locations of loss are. As the depth of loss is not well-constrained (i.e. with Tau depletion profiles) we cannot assume that all loss occurred beneath the in situ attenuation pathlength and instead apply the correction (calculated assuming loss completely beneath the in situ attenuation pathlength) to the uncertainties instead of directly to the average transient erosion rate. However, we assume that none of this affects the meteoric ^{10}Be inventory (if this is what the reviewer means), for the

following reasons: Loss of meteoric ^{10}Be does not need to depend on bulk weathering mass loss, but rather on surface sites available and pH. One extreme example: Assume you dissolve all plagioclase. You will have massive mass loss (Ca, Na, Si) but the clays that form and the Ca-buffered neutral pH ensure that all meteoric ^{10}Be sticks by 100%.

We have changed this paragraph to the following text:

> *"To properly compare the transient denudation rates of Schaller et al. (2009a) with the $^{10}Be_{met}$–derived erosion rates using the methods of von Blanckenburg et al. (2012), the weathering component of denudation must be accounted for. For the Pinedale moraine, chemical weathering mass loss is estimated to be 16% of the denudation rate, while for the Bull Lake moraine, the chemical weathering mass loss accounts for 20% (Schaller et al., 2009b). Assuming that the weathering mass loss took place beneath the cosmic ray attenuation pathway, the recalculated average effective transient erosion rates are then 27.0 mm ky^{-1} and 9.9 mm ky^{-1} for the Pinedale and Bull Lake moraines, respectively. As we have no means to assess whether this assumption is correct, we instead account for this degree of potential loss in the uncertainties (in addition to analytical uncertainties) on the effective transient erosion rates in all further calculations. Regardless, we note that such weathering mass loss does not necessarily need to coincide with loss of dissolved $^{10}Be_{met}$. Rather, the sites of primary mineral dissolution might also be the sites of secondary mineral formation and high dissolved Ca and hence potentially high $^{10}Be_{met}$ retentivity."*

174: This still doesn't clearly state that the two aliquots were combined. Maybe "combined and homogenized".

Revised to "combined and homogenized".

Equation 3: In the previous round, I asked the authors to explicitly add inheritance to this equation. I don't know why they haven't. Explaining something in the text but omitting to include it in formal terms is not enough.

Inheritance corrections are now directly included in Eqs. 2, 3, and 4

Equation 4: The first two terms do not need to be in parentheses. Neither does Iλ (also in eq. 2).

Parentheses removed.

235: So instead of Gaussian, you assume the value is equally likely to fall anywhere within the confidence interval? This doesn't seem justified. You should model the actual probability distribution of each of your values and randomly select from these (if you don't want to solve it analytically).

This is indeed what we previously did, although we have decided to alter our approach as originally suggested by the reviewer in the last round (see below).

For our previous treatment -- yes, Kd values are equally as likely to fall anywhere within the range of values described, with the previous knowledge we have available. For justification -- see below for a plot of Kd values estimated from the Be sorption-desorption experiments from You et al. (1989). The soil profiles analyzed here have an estimated pH of 5.5 at the surface to 8 at depth. Any of these estimates are possible.

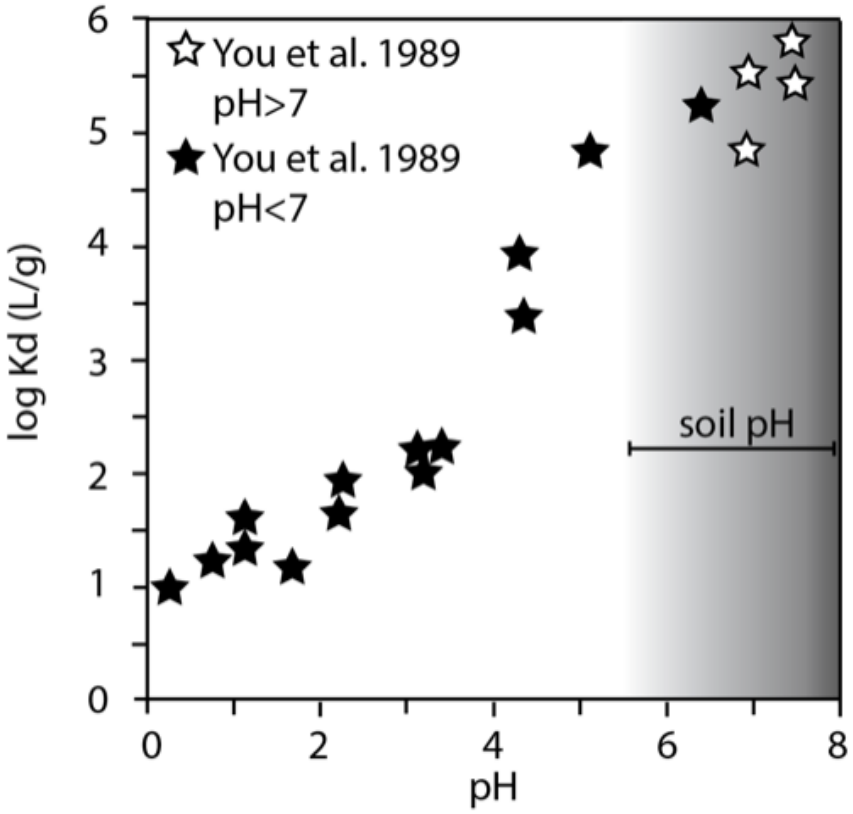

Despite this, it's important to note that uncertainties determined via traditional error propagation, assuming a Gaussian distribution for Kd (and transient erosion rates), for the Pinedale and Bull Lake loss-corrected fluxes are essentially the same as before, now at 1.04 x 10^6 +/- 0.14 at/cm^2/y and 1.04 x 10^6 +/- 0.39 at/cm^2/y, respectively. Please note that these raw (i.e. paleomag-uncorrected) values differ very slightly from the last submission because of the Gaussian treatment. That the estimates are now equal is novel, but unsurprising, given that they previously also agreed very well within error.

We have thus decided to do away with the Monte Carlo entirely, as it makes the determination of uncertainties more complicated than it needs to be to arrive at essentially the same answer. Previously, because we analytically solved (Eq. 4) using an average value for Kd (instead of the median result of the Monte Carlo), we ended up with lopsided uncertainties which is admittedly

confusing (see response below). Since there is no appreciable change in uncertainties with error propagation (nor should there be), the simplest route is the best -- as the reviewer indeed insinuated with the first round of reviews. We have removed all text regarding Monte Carlo-derived uncertainties and have replaced (where necessary) with text describing our error propagation approach.

243: Do you mean 20-40% less than current?

Good catch! This has been corrected.

278: I don't understand why the uncertainties are so lopsided (especially for Pinedale), when the Monte Carlo results are so flat.

This is due to how we use the Monte Carlo -- to only solve for uncertainties, not the reported flux value itself. The median result of the Monte Carlo is not the same result as solving the equation with average values for Kd and erosion rate, which we previously reported.

However, given that determining uncertainties via traditional error propagation gives virtually the same result as the Monte Carlo-derived uncertainties, we have chosen to remove the Monte Carlo from the manuscript and instead report uncertainties using traditional algebraic error propagation.

282: As I mention above, these calculations are in error and need to be excised.

These calculations are not in error - they represent potential maximum bounds for loss. Please see our above justification.

287: I am totally mystified as to why this correction is so large. The records presented in Christl et al., 2010 show very little in the way of variation over the past 25 ka. We need to see the data and equations behind this.

The correction is so large because we must scale for the Holocene after scaling relative to Modern. As shown in Table 3, the scaling factor relative to the modern (determined using Christl et al. 2010, as described in the table) is not that large -- in fact, it's only 1% less than modern for Bull Lake (which is integrated over 24 ky). This is exactly as you describe -- little variation over the past 24 ky.

For the Graly estimate, we cannot use Christl et al. 2010 to normalize to Modern. Instead, we must first recalculate the solar modulation they used (700MV) relative to a phi of 500 MV (this is modern solar modulation value of Steinhilber 2012, which is also used for H&FvB's rescaling in their flux map, by which they then rescale to 280 MV to represent the Holocene average). We do so by utilizing Fig. 4b of Masarik & Beer (2009). The production at 700 MV at this latitude is

0.018 atoms/cm^2/s^1, at 500 MV at this latitude it is 0.022 atoms/cm^2/s^1, dividing the former by the latter gives the production ratio relative to modern of 0.82 for the Graly estimate.

*However, we cannot stop here. We must then scale this value to the Holocene so that *all* flux estimates (including our calculations) agree, otherwise we cannot properly compare between the three flux estimates. This is done by multiplying the scaling factor relative to Modern for our calculations (0.88, 0.99 for Pinedale and Bull Lake) as well as Graly et al. (2011)'s (0.82) by the reciprocal of the scaling factor used by Heikkila and von Blanckenburg (2015) (1.23). This effectively scales all estimates to the average Holocene solar modulation factor of 280.94, as is already done with the estimate from H&FvB. Thus, there are relatively large scaling factors for the production ratio relative to Holocene for our calculated Pinedale and Bull Lake fluxes (0.71 and 0.80), as well as for Graly et al. 2011 (0.67), because the solar modulation is considerably different from Modern (500 MV, using Steinhilber as a modern common reference) to the Holocene-average (280 MV). It is largest for the Graly estimate because we had to scale from 700 MV to 500 MV first, as described above. We finally multiply the calculated or estimated flux by the reciprocal of the production ratio relative to the Holocene*

Please note that there was previously a typo/drafting error for this value for Graly et al. (2011) in column 5 of Table 3. It should be 0.67 (the value used in all calculations). This has been fixed.

We have now added a helpful flow-chart to the Supplemental Material (Fig. S1) that walks the reader through these calculations with a worked example. This will also be helpful to other workers who may need to do paleomagnetic normalizations such as this in the future.

295: This is not true. A linear fit is significantly better for the Bull Lake data (if you exclude the inheritance-dominated samples).

If we were to exclude all samples beneath 60 cm for Bull Lake, a second or third order polynomial is an even better fit -- however, we are referring to the measured depth profile as a whole. We have an expectation of exponential decline for these soil profiles from reactive transport modeling (Maher & von Blanckenburg, 2016) and when considering these profiles wholly we observe this. It's the simplest explanation.

308: Arguably, the bulge may have been missed in the Bull Lake profile, as no sample at equivalent depth was analyzed.

Certainly possible. We make note of this in the text now in this section as follows:

> *It is possible that such an increase may have been missed in the Bull Lake profile, as the equivalent 10cm depth interval was not sampled.*

311-323: I would still like to see this subject treated in more depth. And, I still think that a preference for larger grain sizes in mixing (not downward transport, but mixing) is the most logical explanation.

We have revised the sentence on line 314 and added text to note that while this is a possibility, we don't have enough information to further assess its validity. The text now reads:

> *"The different grain sizes analyzed here and in Schaller et al. (2009a) might exhibit different diffusion coefficients, by which larger grain sizes are more easily mixed, however a trend in smaller grain size fractions with depth within the $^{10}Be_{in\ situ}$ mixing layer would likely be observed if this were the case. Unfortunately, separate grain size classes were not measured for $^{10}Be_{in\ situ}$ within the full mixing zone of either profile to further assess this explanation."*

Line 328: Since you linearly sampled at random from something that varies on an exponential scale, this result is expected. (Though as I mentioned above, I believe this whole term to be in error.)

Given our new error propagation uncertainty treatment, we have removed this sentence describing Monte Carlo simulations. The text now reads:

> *"While the possibility of desorption cannot be ruled out, it's unlikely that either profile has experienced loss to such a degree, as pH, and thus Kd and retentivity, increases with depth. Even in the worst-case scenario of assuming maximum possible loss at the lowest Kd estimate, the magnitude of the potential loss does not substantially affect our calculated $F_{(10Bemet)}$ estimates within uncertainties. Our calculations thus capture the potential maximal bound for loss via propagated uncertainties."*

Line 345: I don't know why you took out the +20% paleo-precipitation from (Birkel et al., 2012). I thought that was a very useful point to bring in. My previous review stated only that you could not meaningfully use it as an upper bound when comparing the Graly et al. value to your results. Quoting the highest regional precipitation rate seems far less useful a fact than a paleo-precipitation model result.

We quote a higher precipitation rate not to place an upper bound on the Graly et al. (2011) estimate for this local site, but to highlight that within the same region/cell covered by the Heikkila and von Blanckenburg (2015) estimate, substantial local differences in average precipitation exist. This leads to estimates that considerably differ for localities using Graly (local precip. input) compared to H&FvB (regional). Within the area contained by the grid cell, the former estimate can scale considerably based on precipitation input, while the latter will always be the same. This is an important point that future workers should consider when estimating meteoric ^{10}Be fluxes, particularly in study areas nearby mountain ranges/precipitation gradients. We make this clearer by adding to the text as follows:

> *For example, if one were to estimate $F_{(10Bemet)}$ from Graly et al. (2011) via (Eq. 1) to nearby Fish Lake Mountain contained within the same Heikkilä and von Blanckenburg (2015) grid cell as this study site, with a modern precipitation rate of 128 cm y^{-1} (WRCC, 2005), the $F_{(10Bemet)}$ would be 2.5 x 10^6 atoms cm^{-2} y^{-1}, substantially higher than that predicted from Heikkilä and von Blanckenburg (2015).*

The +20% paleo-precipitation rate was previously applied directly to our calculations, which is overly credulous to Birkel et al. (2012)'s coarse-resolution modeled results that might not be applicable to this low elevation site in the Wind River mountains. This is a separate discussion point -- that paleo-precipitation may have been higher at this particular site does not serve to illustrate that the region covered by a grid cell of Heikkila and von Blanckenburg (2015) is large and can include areas with substantial precipitation gradients that would give rise to different flux estimates between methods (as we see here).

Table 1: The final column should have inheritance subtracted.

Agreed, this has been fixed both here and in the reporting of calculated inventory values in section 4.1.

Table 3: Uncertainties must be included for the Graly et al. (2011) line of this table. A root mean square error is provided in the publication.

Indeed! This has been fixed, thanks for pointing it out.

I have no idea how the 0.83 value for the Graly et al. (2011) Holocene F term is derived. It is certainly not the first column divided by the third column, as the others seem to be. I am equally mystified as to how the Holocene correction factor for the Graly line is derived.

There is an unfortunate typo/drafting error here. The correction factor relative to Holocene should be 0.665 (rounded to 0.67), not 1.06. The typo value of 1.06 was never used in any calculation. This has been fixed. This scaling factor is calculated by dividing the Graly scaling factor relative to Modern (0.82) by the Heikkila scaling factor relative to Modern (1.23) for a value of 0.67. Then, we divide the calculated flux (0.55) by this value (0.67) to arrive at a rescaled flux of 0.83E6 at/cm^2/y.

The Heikkilä line must also have uncertainties. These are provided in the publication. The industrial run is not an uncertainty. It is a different result.

We previously phrased this poorly in the footnote -- this is now changed (thanks for pointing this out):

> *[d] uncertainty represents the difference between the 'industrial' and the "pre-industrial" modeled flux of Heikkilä and von Blanckenburg (2015)*

Reviewer 2

I just have a few suggestions for minor edits prior to publication.

On line 87, the grain size fraction should be <2 um.

Fixed, thank you.

In the results section, the authors should refer to the equations they used to calculate the inventory values.

Done.

Table 2 is the first table reference in the text, so it should probably be renumbered to Table 1. Alternatively, this table could go into the supplementary material.

Good catch, this has been changed.

Calibrating a long-term meteoric ^{10}Be delivery rate into eroding Western US glacial deposits by comparing meteoric and in situ-produced ^{10}Be depth profiles

Travis Clow[1], Jane K. Willenbring[1,2], Mirjam Schaller[3], Joel D. Blum[4], Christl, M.[5], Peter W. Kubik[5], Friedhelm von Blanckenburg[2]

[1]Department of Geological Sciences, Stanford University, Stanford, CA, USA
[2]GFZ German Research Centre for Geosciences, Earth Surface Geochemistry, Telegrafenberg, 14473 Potsdam, Germany
[3]Geodynamics, University of Tübingen, Wilhelmstraße 56, 72076 Tübingen, Germany
[4]Department of Earth and Environmental Sciences, University of Michigan, Ann Arbor, MI, USA
[5]ETH Zurich, Laboratory of Ion Beam Physics, HPK G23, Schafmattstrasse 20, ETH-Zurich, CH-8093 Zurich, Switzerland

Correspondence to: Travis Clow (tclow@stanford.edu)

Abstract. Meteoric ^{10}Be (^{10}Be$_{met}$) concentrations in soil profiles have great potential as a geochronometer and a tracer of Earth surface processes, particularly in fine-grained soils lacking quartz that would preclude the use of *in situ*-produced ^{10}Be (^{10}Be$_{in\ situ}$). One prerequisite for using this technique for accurately calculating rates and dates is constraining the delivery, or flux, of ^{10}Be$_{met}$ to a site. However, few studies to date have quantified long-term (i.e. millennial) delivery rates, and none have determined a delivery rate for an eroding soil. In this study, we compared existing concentrations of ^{10}Be$_{in\ situ}$ with new measurements of ^{10}Be$_{met}$ in eroding soils sampled from the same depth profiles to calibrate a long-term ^{10}Be$_{met}$ delivery rate. We did so on the Pinedale (~21-25 ky) and Bull Lake (~140 ky) glacial moraines at Fremont Lake, Wyoming (USA) where age, grain sizes, weathering indices, and soil properties are known, as are erosion/denudation rates calculated from ^{10}Be$_{in\ situ}$. After ensuring sufficient beryllium retention in each profile, solving for the delivery rate of ^{10}Be$_{met}$, and normalizing for paleomagnetic and solar intensity variations over the Holocene, we calculate ^{10}Be$_{met}$ fluxes of 1.46 (± 0.20) x 10^6 atoms cm^{-2} y^{-1} and 1.30 (± 0.48) x 10^6 atoms cm^{-2} y^{-1} to the Pinedale and Bull Lake moraines, respectively, and compare these values to two widely-used ^{10}Be$_{met}$ delivery rate estimation methods that substantially differ for this site. Accurately estimating ^{10}Be$_{met}$ flux using these methods requires consideration of spatial scale as well as temporally varying parameters (i.e. paleomagnetic field intensity, solar modulation) to ensure the most realistic estimates of ^{10}Be$_{met}$-derived erosion rates in future studies.

Deleted: to the Holocene-average

Deleted: 52 (+

Deleted: 11/-0.21

Deleted: 31 (+

Deleted: 43/-0.50

1 Introduction

^{10}Be is a cosmogenic isotope with a half-life of 1.39 +/- 0.01 My (Chmeleff et al., 2010) and its meteoric form ($^{10}Be_{met}$) is produced in the atmosphere through spallation reactions as high-energy cosmic rays collide with target nuclei (i.e. ^{14}N and ^{16}O) in the atmosphere (Lal and Peters, 1967). $^{10}Be_{met}$ is then delivered to Earth's surface via precipitation or as dry deposition at a flux of 0.1 – 2 x 10^6 atoms cm^{-2} y^{-1} followed by dissolved export in runoff, or depending on retentivity, adsorption onto fine-grained, reactive surfaces, typically clays and Fe- and Al-oxyhydroxides in soil horizons at the Earth's surface (Graly et al., 2010; Willenbring and von Blanckenburg, 2010). $^{10}Be_{met}$ has been used as a tracer of Earth surface processes, including estimating erosion rates at the soil-profile and river-catchment scales, soil residence times, ages of landforms over millennial to million-year timescales, and paleo-denudation rates from marine sedimentary records (Pavich et al., 1986; McKean et al., 1993; Jungers et al., 2009; Willenbring and von Blanckenburg, 2010; von Blanckenburg et al., 2012; von Blanckenburg and Bouchez, 2014; Wittman et al., 2015; von Blanckenburg et al., 2015; Portenga et al., 2019; Jelinski et al., 2019). Prerequisites for interpreting the concentrations and isotope ratios (i.e. $^{10}Be_{met}/^{9}Be$) as erosion or denudation (the sum of erosion and weathering) rates, respectively, include knowing the delivery rate of $^{10}Be_{met}$ (Pavich et al., 1986; Reusser et al., 2010; Graly et al, 2011; Heikkilä and von Blanckenburg, 2015; Dixon et al., 2018, Deng et al., 2020) and quantifying the mobility or retention of beryllium in soils (e.g. Bacon et al., 2012; Boschi and Willenbring, 2016a,b; Maher and von Blanckenburg, 2016; Dixon et al., 2018), not all of which was possible in many previous studies. The potential ability of using $^{10}Be_{met}$ depth profiles to obtain quantitative data on soil ages, residence times, production- and denudation rates in a similar manner as *in situ*-produced ^{10}Be ($^{10}Be_{in\ situ}$) depth profiles could prove to be highly advantageous, as it is easier to measure (due to much higher concentrations than $^{10}Be_{in\ situ}$) and can be employed in a much wider range of environments, as there is no dependence on the existence of coarse-grained quartz as is required for the analysis of $^{10}Be_{in\ situ}$. $^{10}Be_{in\ situ}$ shares a cosmic ray origin with $^{10}Be_{met}$ but differs in production method; $^{10}Be_{in\ situ}$ is produced within crystal lattices in surface rocks and soil, rather than in the atmosphere, with a well constrained total production rate of 4.01 atoms $g^{-1}y^{-1}$ at sea level, high latitude (Borchers et al., 2016), and is characterized by full retentivity and known production pathways with depth. $^{10}Be_{met}$, in stark contrast, is potentially subjected to variable adsorption depths, incomplete retentivity, and heterogeneous internal redistribution.

In this study, we compare the previously published $^{10}Be_{in\ situ}$ depth profiles of the Pinedale and Bull Lake terminal glacial moraines in Wind River, Wyoming (Schaller et al., 2009a,b) with new $^{10}Be_{met}$ concentrations from depth profiles from the same sample material to evaluate the long-term (i.e. millennial) delivery rate of $^{10}Be_{met}$ ($F_{(^{10}Be_{met})}$) to this site. This is the first study that evaluates $F_{(^{10}Be_{met})}$ for eroding soils as derived from the comparison of $^{10}Be_{in\ situ}$ and $^{10}Be_{met}$ depth profiles and erosion rates. We utilize previous knowledge of effective transient erosion rates from Schaller et al. (2009a), recalculated with revised parameters for *in situ* production of ^{10}Be, to constrain and locally calibrate $F_{(^{10}Be_{met})}$ to these moraines while considering the extent of $^{10}Be_{met}$ retention post-delivery. We then compare the resulting calculated $F_{(^{10}Be_{met})}$, with propagated uncertainties, with the predicted $F_{(^{10}Be_{met})}$ of Graly et al. (2011) and Heikkilä and von Blanckenburg (2015), normalizing each result for paleomagnetic field intensity variations over the Holocene. We also explore the practical differences between these flux estimates and advocate for each approach to be carried out when estimating $F_{(^{10}Be_{met})}$ for use in erosion rate calculations in future studies.

Deleted: determined via Monte Carlo simulations

2 Background

2.1 Study Area

The Fremont Lake area of the Wind River Mountains (Wyoming, United States) experienced multiple glacial advances during the Pleistocene, evidenced by several moraines of Pinedale and Bull Lake age (Fig. 1; modified from original mapping and descriptions by Richmond, 1973). The climate is cold, semi-arid, and windy, with a 50-year precipitation rate and temperature of 27.6 cm y^{-1} and 2.1° C, respectively (WRCC, 2005), in the nearby town of Pinedale, Wyoming (~3.5 km southwest of the field area).

The Pinedale and Bull Lake age terminal moraines (hereafter referred to as Pinedale and Bull Lake moraines) analyzed in this study (Fig. 1) were formed by highland-to-valley mountain glaciers draining an ice cap accumulation zone that covered the mountain range. The Pinedale moraine is more steep-sided and boulder-strewn than the gently sloping Bull Lake

moraine, each with a total height of ~30 m (see Figs. 1b, 1c of Schaller et al., 2009a for detailed moraine transects). The pH of the moraine soils is well characterized; both profiles have pedogenic carbonate below 1 m, fixing the pH at depth to ~ 8 (Chadwick and Chorover, 2001). Hall and Shroba (1995) report pH data on profiles adjacent to those analyzed in this study, with average pH ranging from ~5.5 on the surface to ~8 at depth.

The depth profile samples analyzed for $^{10}Be_{met}$ reported here are the same sample material analyzed for $^{10}Be_{in\ situ}$ by Schaller et al. (2009a). We utilize bulk samples sieved to <2 mm for our analysis, extracted from the lower mineral soil developed on each moraine, both mixtures of reworked glacial till (composed of Archean granite, granodiorite, and dioritic gneiss) that have a high likelihood for inheritance from cosmic ray exposure prior to burial. The same reported depths and grain size distributions apply for each sample at depth. The primary mineral content in the deepest (unweathered, >2 mm size fraction) sample is (in order of decreasing abundance): plagioclase, quartz, biotite, K-feldspar, hornblende, and magnetite (Taylor and Blum, 1995). Secondary clay minerals in the ≤2 μm size fraction include kaolinite, vermiculite, illite, and smectite (Mahaney and Halvorson, 1986), with total clay content ranging from 3 to 10 wt% and 9 to 30 wt% for the Pinedale and Bull Lake profiles, respectively. Major element data is reported in Schaller et al. (2009b). Sr isotope measurements of the moraine soils and dust sources showed insignificant dust fluxes in the depth profiles of the Pinedale and Bull Lake moraines (Blum and Erel, 1997; Taylor and Blum, 1997).

2.2 Independent $^{10}Be_{met}$ Flux Estimation

Accurately estimating $F_{(^{10}Be_{met})}$ from field experiments is a topic of ongoing debate (e.g. Ouimet et al., 2015; Dixon et al., 2018), particularly in regard to the effect of precipitation rate on the flux (i.e. whether precipitation leads to additive or dilution effects on delivered $^{10}Be_{met}$, see *Willenbring and von Blanckenburg (2010)* and *Deng et al. (2020)* for extensive reviews). $F_{(^{10}Be_{met})}$ also varies through time, depending on solar modulation and paleomagnetic field intensity, and has a spatial distribution primarily resulting from atmospheric mixing and scavenging. One means to estimate $^{10}Be_{met}$ production and delivery are $F_{(^{10}Be_{met})}$ estimates based on global atmospheric models (Field et al., 2006; Heikkilä and von Blanckenburg, 2015), which provide an estimate over large spatial scales. Another type of estimate is based on empirical, precipitation-

dependent field estimates of $^{10}Be_{met}$ inventories in dated soils (Graly et al., 2011) measured over annual time scales. The work of Ouimet et al. (2015) highlighted the necessity for local $F_{(^{10}Be_{met})}$ estimates that also integrate over millennial time scales against models such as these, as their comparison of $^{10}Be_{met}$ inventories and deposition rates from Pinedale- and Bull Lake-aged landforms in the Colorado Front Range showed that some were lower, and some exceeded, deposition rates from atmospheric models and precipitation collections.

The $F_{(^{10}Be_{met})}$ map of Heikkilä and von Blanckenburg (2015) utilizes the $^{10}Be_{met}$ production functions of Masarik and Beer (1999) combined with the ECHAM5 general circulation model (GCM). Production rates were scaled to reflect the solar modulation and magnetic field strength for the entire Holocene (280.94 MV) using measured ^{10}Be concentrations in ice cores. The authors ultimately present a global grid of predicted "pre-industrial" and "industrial" (referring to simulated aerosol and greenhouse gas concentrations) Holocene $F_{(^{10}Be_{met})}$ with an approximate cell size of 300 km x ~230 km. GCMs such as this are useful for modeling atmospheric mixing of $^{10}Be_{met}$, particularly in the stratosphere, as well as the regional effect of climate and its influence on $F_{(^{10}Be_{met})}$ via atmospheric circulation and precipitation (Heikkilä et al., 2012). At this latitude (~42.9° N), the pre-industrial predicted $F_{(^{10}Be_{met})}$ of 1.38 x 10^6 atoms cm^{-2} y^{-1} is nearly identical to that derived from the flux map of Field et al. (2006), which utilizes the GISS (Goddard Institute for Space Studies Model E) GCM to model production. We use the pre-industrial modeled $F_{(^{10}Be_{met})}$ in our comparisons, as it is a more appropriate estimate for landforms of these ages. To place an upper bound uncertainty on this estimate, which is otherwise hard to quantify, we utilize the difference between the industrial and pre-industrial predicted $F_{(^{10}Be_{met})}$ (+0.99 x 10^6 atoms cm^{-2} y^{-1}). This difference is solely a result of climate-dependent shifts in the delivery of $^{10}Be_{met}$ and shifts resulting from large industrial aerosol loading in modern times and does not reflect changes in atmospheric production (Heikkilä and von Blanckenburg, 2015).

Deleted: modelling

Deleted: While

Deleted: applicable for comparison

Deleted: of 2.37

Deleted: as an upper bound uncertainty on their estimate.

On the other hand, the empirical, present-day estimates of $F_{(^{10}Be_{met})}$ from Graly et al. (2011) are based on measurements of $^{10}Be_{met}$ deposition rates from contemporary measurements of $^{10}Be_{met}$ in precipitation, corrected for dust and normalized to a modern (1951-2004) solar modulation value (700 MV). A first order estimate of the $F_{(^{10}Be_{met})}$ was empirically derived given latitude (L) and average precipitation rate (P) to the study area (Graly et al., 2011):

$$F_{(^{10}\mathrm{Be_{met}})} = P \times (1.44 / (1 + \mathrm{EXP}((30.7 - L) / 4.36)) + 0.63) \quad (1)$$

Uncertainty for this type of estimate can be determined using the root mean square error (1.75 x 10^3 atoms cm^{-3}) of the resultant latitudinal trend in predicted $F_{(^{10}Be_{met})}$ (see Fig. 5 of Graly et al. 2011). A predicted $F_{(^{10}Be_{met})}$ of 0.55 (± 0.05) x 10^6 atoms cm^{-2} y^{-1} is calculated for these Wind River moraines using (Eq. 1), however in order to compare these two estimates with each other, as well as to our calculated $F_{(^{10}Be_{met})}$, we later normalize them all to a common paleomagnetic and solar intensity datum (i.e. the Holocene).

Deleted: A predicted $F_{(^{10}Be_{met})}$ of 0.55

3 Methods

3.1 Recalculating Previous Age Constraints

Ages for each moraine have been independently determined via multiple methods, with $^{10}Be_{in\ situ}$ surface exposure ages of boulders combined with ^{230}Th/U ages of nearby contemporaneous fluvial terraces yielding the most reliable average estimates of 21 ky and 140 ky for the Type-Pinedale and Bull Lake-age moraines, respectively (Gosse et al., 1995; Phillips et al., 1997; Easterbrook et al., 2003; Sharp et al., 2003). These ages closely correspond with global maximum ice volumes of marine oxygen isotope stages 2 and 6, respectively (Sharp et al., 2003). We recalculated the ^{10}Be boulder surface exposure ages used to constrain the timing of advancement of each moraine to its terminal position based on a recent revision of the ^{10}Be half-life, which affected the AMS standard values (Chmeleff et al., 2010), and the most recent nucleonic production rate of 3.92 atoms g^{-1} y^{-1} at sea level-high latitude (Borchers et al., 2016) (Table S1); the updated independent age constraints are 25 ky for the Pinedale moraine and remain at 140 ky for the Bull Lake moraine (see Supplementary Material for details).

3.2 Recalculating Previous Denudation Constraints

All moraine surfaces have been eroded to some extent after their deposition. To estimate the amount of erosion for our calculations, we utilize the previously reported denudation rates (comprising erosion and chemical loss by dissolution) for the Pinedale and Bull Lake moraines (Schaller et al., 2009a) from the same depth profiles and material analyzed in this study. The denudation rates of Schaller et al. (2009a) were calculated using a sea level, high latitude production rate of 5.1 atoms $g_{(qtz)}^{-1}$ y^{-1} (Stone, 2000) and a decay constant of 4.62 x 10^{-7} y^{-1}. Denudation rates were recalculated using CRONUS v.3 (Phillips et al., 2016) with the updated half-life and production rate values (Table S1) and updated independent age constraints scaled to the sample altitude and latitude (Dunai, 2000) assuming two denudation rate scenarios: one of constant denudation since moraine deposition, and the other of transient denudation decreasing in magnitude since moraine deposition. Recalculated average denudation rates are 32.1 ± 2.7 mm ky^{-1} and 12.4 ± 4.8 mm ky^{-1} for the Pinedale and Bull Lake moraines, respectively, in the case of transient denudation, and are 15 mm ky^{-1} and 7.5 mm ky^{-1} for the Pinedale and Bull Lake moraines, respectively, in the case of constant denudation (Table 1). These recalculated denudation rates are determined from the best-fit Chi-Square solutions obtained from running Models 2, 4, 6, and 8 of Schaller et al. (2009a) with present-day parameters (See Supplementary Material for details). We consider the transient denudation rates to more closely approximate reality, as moraines, deposited as ~triangular landforms at the terminus of glaciers, initially experience faster denudation than that towards present day, where the moraines evolve to a concave-down parabolic geometry. As the curvature of the topography reduces over time, hillslope diffusion law dictates that the denudation rates will decrease as the moraine flattens. This approach integrates this transient behavior over the entire age of each moraines, and thus likely overstates the loss of ^{10}Be to erosion to some degree, however it nonetheless provides the most realistic estimates possible for these moraines as we are otherwise unable to independently constrain their site-specific erosion rates.

To properly compare the transient denudation rates of Schaller et al. (2009a) with the $^{10}Be_{met}$–derived erosion rates using the methods of von Blanckenburg et al. (2012), the weathering component of denudation must be accounted for. For the Pinedale moraine, chemical weathering mass loss is estimated to be 16% of the denudation rate, while for the Bull Lake moraine, the chemical weathering mass loss accounts for 20% (Schaller et al., 2009b). Assuming that the weathering mass

Deleted: 2

Deleted: If

loss took place beneath the cosmic ray attenuation pathway, the recalculated average effective transient erosion rates are then 27.0 mm ky^{-1} and 9.9 mm ky^{-1} for the Pinedale and Bull Lake moraines, respectively. As we have no means to assess whether this assumption is correct, we instead account for this degree of potential loss in the uncertainties (in addition to analytical uncertainties) on the effective transient erosion rates in all further calculations. Regardless, we note that such weathering mass loss does not necessarily need to coincide with loss of dissolved $^{10}Be_{met}$. Rather, the sites of primary mineral dissolution might also be the sites of secondary mineral formation and high dissolved Ca ensuing circumneutral pH and hence potentially high $^{10}Be_{met}$ retentivity.

Deleted: there is
Deleted: way
Deleted: where
Deleted: mass loss occurred
Deleted: utilize
Deleted: to place

3.3 $^{10}Be_{met}$ Analysis

We analyzed approximately 1-2 g aliquots of the <2 mm grain-size moraine sediment fraction from the same ~10-15 cm depth intervals as Schaller et al. (2009a) analyzed for Be isotope abundance at the Laboratory for the Geochemistry of the Earth Surface at GFZ Potsdam. We followed the sediment leaching procedure described in Ebert et al. (2012) and Wittmann et al. (2012), which was adapted from Bourlés (1988) and Guelke-Stelling and von Blanckenburg (2012), to extract Be isotopes from outer grain surfaces. Bulk samples underwent two steps to remove the adsorbed beryllium: a 24-hr agitation in 0.5 M HCl (to extract amorphous oxide-bound Be), and 1 M hydroxylamine-hydrochloride (to remove crystalline-bound Be). After each step, the supernate was separated from the sediment.

Deleted: .

To measure the adsorbed $^{10}Be_{met}$, the two aliquots of leached material were combined and homogenized with ~200 µg of ^{9}Be carrier (Table 2) and 2 mL HF was added to the acid sample solution. This solution was nearly completely dried down and then dissolved in 1 additional mL of 50% HF acid and dried down completely, repeated once. We then added 10 mL ultrapure (18 MΩ) water to the warm fluoride residue and leached it for 1 h on a warm hotplate. The water containing the Be was gently removed via pipette and dried down separately. The Be in the water leach solution was extracted and purified by a form of the ion exchange chromatography procedure from von Blanckenburg et al. (2004) that was adapted for $^{10}Be_{met}$ purification by passing the leachate through anion (2 ml of BioRad 1x8 100-200 mesh resin) and cation (2x 1 ml BioRad AG50-X8 200-400 mesh) exchange resins, precipitated at pH ~9 using $NH_4OH:H_2O$ (1:1), washed twice with 2 ml ultrapure water with centrifugation in between, mixed with AgCl, centrifuged and dried overnight, and finally oxidized over open

Deleted: µl
Deleted: 1
Deleted: meteoric ^{10}Be

flame (>1000 °C; modified from Kohl & Nishiizumi, 1992). $^{10}Be_{met}/^{9}Be$ ratios were measured at the Zurich AMS Lab (Kubik and Christl, 2010) (S555 standard, nominal $^{10}Be/Be = 95.5 \times 10^{-12}$), from which the ^{10}Be concentration ($^{10}Be_{reac} = {}^{10}Be_{met}$) was calculated. Two carrier blanks analyzed with the samples register AMS $^{10}Be/^{9}Be$ ratios of $3.2 \pm 1.5\times10^{-15}$, and $2.2 \pm 1.5\times10^{-15}$ containing ≪0.1% of the ^{10}Be in analyzed samples.

3.4 $^{10}Be_{met}$ Flux Calculations

In an actively eroding setting, erosion rates can be calculated with knowledge of 1) the total inventory of $^{10}Be_{met}$ in the depth profile, 2) a known/estimated $^{10}Be_{met}$ flux to the location, 3) the $^{10}Be_{met}$ retention behavior, and 4) an assumption of approximate steady state conditions, which is only justified if the inventory of $^{10}Be_{met}$ is independent of the initial exposure age of the soil. Here, steady state means that $^{10}Be_{met}$ lost through erosion and decay equals the $^{10}Be_{met}$ gained from atmospheric flux (e.g. Brown et al., 1988; Willenbring and von Blanckenburg, 2010), a prerequisite of which is that the residence time of soil material containing $^{10}Be_{met}$ with respect to erosion is much less than the depositional age (Willenbring and von Blanckenburg, 2010), which holds true for these moraines. For an assumed steady state inventory, the inverse relationship between the local erosion rate and the $^{10}Be_{met}$ content in the soil profile is exploited to determine a flux of $^{10}Be_{met}$ using the formulation of Brown (1987), rearranged as follows:

$$F(^{10}Be_{met}) = E \times ([^{10}Be]_{reac} - [^{10}Be]_{inher}) + I\lambda \quad (2)$$

Where E is the erosion rate [g cm^{-2} y^{-1}], $F(^{10}Be_{met})$ is the atmospheric flux of $^{10}Be_{met}$ [atoms cm^{-2} y^{-1}], $[^{10}Be]_{inher}$ is the inherited nuclide concentration [atoms cm^{-2}], I is the inheritance-corrected inventory of $^{10}Be_{met}$ [atoms cm^{-2}] in the depth profile, λ is the decay constant of ^{10}Be [y^{-1}], $[^{10}Be]_{reac}$ is the $^{10}Be_{met}$ concentration at the surface of the soil [atoms g^{-1}]. Inventories were calculated following Willenbring and von Blanckenburg (2010) using a depth-averaged regolith density (ρ) of 2.0 g cm^{-3} for each profile (Schaller et al., 2009a,b), where z is the depth to the bottom of the soil column and $([^{10}Be]_{reac}(z) - [^{10}Be]_{inher})$ is the concentration of $^{10}Be_{met}$ at depth, minus inheritance:

Deleted: meteoric ^{10}Be

Deleted:).

Deleted: × [^{10}Be]

Deleted: + (

Deleted:) → → → → → → →

Deleted: inheritance-corrected

Deleted: [

$$I = \int_0^z ([^{10}Be]_{reac(z)} - [^{10}Be]_{inher})\rho dz \quad (3)$$

Deleted: $\int_0^z [^{10}Be]_{reac}(z)\rho dz$

Both $^{10}Be_{met}$ and $^{10}Be_{in\ situ}$ depth profiles show indications of inherited nuclide concentrations at depth, likely due to incomplete glacial erosion resetting for each moraine (Schaller et al., 2009a) and exposure to $^{10}Be_{met}$ during or immediately after glacial processes. Higher concentrations at depth are observed for the Bull Lake moraine for both nuclide profiles (Fig. 1, Table 2), potentially due to the presence of pre-irradiated reworked till. We consider the lowest concentration observed for each depth profile as $[^{10}Be]_{inher}$ and subtract it from all measured concentrations.

Deleted: 2009a).

Deleted: 1

Deleted: the inherited $^{10}Be_{met}$ concentration

Desorption of $^{10}Be_{met}$ can affect the inventory of $^{10}Be_{met}$ when erosion rates are low, water flux is high and soil chemistry favors mobility. Given that for these soil profiles pH ranges from 8 at depth to ~5.5 at the surface (Hall and Shroba, 1995), we must consider incomplete retention of beryllium and thus a reduced inventory and surface concentration used in (Eq. 2) (Bacon et al., 2012; Maher and von Blanckenburg, 2016). Applying a correction directly to the calculation of $^{10}Be_{met}$ flux is possible via a combination of (Eq. 2) (this study) and (Eq. 3) of von Blanckenburg et al. (2012), which requires an accurate estimation of the water flux out of the system (Q) and the Be partition coefficient (K_d).

Deleted: between

Deleted: and

$$F(^{10}Be_{met}) = E \times ([^{10}Be]_{reac} - [^{10}Be]_{inher}) + I\lambda + Q \times ([^{10}Be]_{reac} - [^{10}Be]_{inher}) \div K_d \quad (4)$$

Deleted: = (

Deleted: × $[^{10}Be]$

Deleted: + (Iλ)) +

Deleted: $[^{10}Be]$

Deleted: ÷

K_d is estimated as 1 x 10^5 to 1 x 10^6 L kg^{-1} (with an average of 5.5 x 10^5 L kg^{-1}) from the surficial pH of ~5.5 to ~8 at depth via Be sorption-desorption experiments from You et al. (1989). We estimate Q by proxy via the modern precipitation rate of 276 L m^{-2} y^{-1}.

Utilizing (Eq. 4) and previous knowledge of the effective transient erosion rates, we calculate the loss-corrected $F(^{10}Be_{met})$ to the locations of these moraines. To further account for the full range of possible K_d values and transient erosion rates, we use traditional algebraic error propagation to determine the uncertainty of the calculated fluxes.

Deleted: employ Monte Carlo simulations

3.6 Normalizing flux estimates for cosmic ray intensity variations over the Holocene

Geomagnetic field strength has varied considerably from the late Pleistocene to present and exerts the primary quantifiable influence on temporal variability in the production rate of cosmogenic nuclides in an inverse fashion (Pigati and Lifton, 2004). Relative paleointensity over the last 140 ky is, on average, ~20-40% less than the current geomagnetic intensity depending on the methodology employed (e.g. Frank et al., 1997; Valet et al., 2005). The flux map of Heikkilä and von Blanckenburg (2015) accounts for paleomagnetic field and solar intensity variations over the Holocene via the reconstruction method of Steinhilber et al. (2012), which effectively increases the production rate used in their model by 1.23 times the present-day rate by rescaling the modern solar modulation factor (500 MV) and associated geomagnetic field intensity to that of the Holocene average (280.94 MV). As the estimations of flux from Graly et al. (2011) were normalized to reflect a solar modulation of 700 MV, we rescaled the modern Graly-derived $F_{(^{10}Be_{met})}$ to the average Holocene solar modulation factor of 280.94 MV used in the flux map of Heikkilä and von Blanckenburg (2015) following the paleomagnetic and solar intensity normalization procedure of Deng et al. (2020). This is carried out by first rescaling production at 700 MV to 500 MV (i.e. the modern solar modulation factor of Steinhilber et al., (2012)) via Fig. 4B of Masarik & Beer (2009) for a Graly et al. (2011)-specific modern production ratio of 0.82 (Table 3). Then, to properly normalize for the Holocene, we multiply this modern production ratio by the reciprocal of the rescaling production ratio of Heikkilä and von Blanckenburg (2015) (1.23) to arrive at a Holocene-normalized production ratio of 0.67 and apply this to the Graly et al. (2011) flux estimate (Table 3). We illustrate and further describe the details of this procedure in the Supplementary Material (Fig. S1).

To further compare the model- and the precipitation-derived Holocene-average $F_{(^{10}Be_{met})}$ estimates with those calculated in this study, we must also normalize for geomagnetic and solar intensity variations within the Holocene (for Pinedale, with a 6 ky cosmogenic integration time) and beyond the Holocene (for Bull Lake, with a 24 ky cosmogenic integration time). We again linearly rescaled our calculated loss-corrected $F_{(^{10}Be_{met})}$ for the Pinedale and Bull Lake moraines by first integrating the production rate relative to the modern using the Principle Component 1 (PC1) of the ^{10}Be marine core record of Christl et al. (2010), converting PC1 into relative fluxes from 6 ky and 24 ky, respectively, and then normalizing these values to those over the Holocene, propagating the statistical uncertainties. These time intervals represent the calculated

Deleted: ¶
3.5 Monte Carlo Simulations¶
To assess the uncertainties of the calculated flux estimates, Monte Carlo simulations were used to solve for $F_{(^{10}Be_{met})}$ via (Eq. 4) over the entire range of possible values for each term (Table 3) for the Pinedale and Bull Lake moraines. This method is advantageous compared to traditional algebraic error propagation as it doesn't assume a Gaussian distribution, nor does it require an average K_d value input for each moraine, which is difficult to estimate accurately. We carry out each Monte Carlo simulation over 100,000 iterations and report uncertainties representing the 95% confidence intervals of each simulation. The MATLAB code used for these simulations is available in the Supplementary Material.¶

Deleted: geomagnetic

Deleted: of

Deleted: Phi

Deleted: 94MV

Deleted: via Masarik and Beer (2009) and Steinhilber et al. (2012), …

Deleted: (2020

Deleted: properly

Deleted: for the Holocene. We

Deleted: transport-corrected

Deleted:)

Deleted: from the Monte Carlo simulations.

residence/integration times of the soil profiles from the surface to the e-folding adsorption depth of $^{10}Be_{met}$ (20 and 30 cm for the Pinedale and Bull Lake moraines, respectively). This approach accounts for the cumulative effects of transient erosion and leaching by weighting geomagnetic intensity variations on $F_{(^{10}Be_{met})}$ towards the present.

4 Results

4.1 Meteoric Cosmogenic ^{10}Be Concentrations

The measured $^{10}Be_{met}$ concentrations are reported along with the previously published $^{10}Be_{in\ situ}$ concentrations (Schaller et al., 2009a) for the Pinedale and Bull Lake profiles (Table 2); $^{10}Be_{met}$ depth profiles are presented for the Pinedale and Bull Lake profiles in Figure 2. The Pinedale depth profile has $^{10}Be_{met}$ concentrations ranging from 3.57 (± 0.32) to 199.53 (± 5.26) x 10^6 atoms g^{-1}. The highest nuclide concentration is measured at 10 cm, rather than at the surface. Below this maximum value, concentrations decrease exponentially until reaching an asymptote at ~ 3 to 6 x 10^6 atoms g^{-1} from 43 cm to the bottom of the profile (180 cm), the lowest of which we consider to be an inherited component. The Pinedale depth profile has a calculated, inheritance-corrected inventory (Eq. 3) of 5387 (± 122) x 10^6 atoms cm^{-2}.

The Bull Lake depth profile has $^{10}Be_{met}$ concentrations ranging from 6.32 (± 0.25) to 415.48 (± 12.46) x 10^6 atoms g^{-1}. The highest nuclide concentration is measured at the surface; below this, concentrations decrease in an approximately exponential fashion until reaching an asymptote at ~ 6 to 8 x 10^6 atoms g^{-1} from 64 cm to the bottom of the profile (130 cm), the lowest of which we also consider to be an inherited component. The Bull Lake depth profile has a calculated, inheritance-corrected inventory (Eq. 3) of 17310 (± 318) x 10^6 atoms cm^{-2}. The $^{10}Be_{met}$ inventory from the Bull Lake moraine is roughly 3 times higher than that of the Pinedale moraine.

4.2 $^{10}Be_{met}$ Fluxes

The loss-corrected $F_{(^{10}Be_{met})}$ as calculated from (Eq. 4) is 1.04 (± 0.14) x 10^6 atoms cm^{-2} y^{-1} and 1.04 (± 0.39) x 10^6 atoms cm^{-2} y^{-1} for the Pinedale and Bull Lake moraines, respectively (Table 3), with uncertainties determined via traditional algebraic error propagation, assuming a Gaussian distribution for the estimated K_d and transient erosion rate values.

Deleted: 1

Deleted: an

Deleted: 6672

Deleted: the

Deleted: an

Deleted: 19021

Deleted: 08 (+

Deleted: 10/-0.16

Deleted: 05 (+

Deleted: 35/-0.40

Deleted: where the Monte Carlo-derived

Deleted: reflect the 95% confidence interval of all possible input parameters

Retention calculations from (Eq. 4) across the entire range of possible K_d values indicate that the potential desorption loss at the surface of the Pinedale and Bull Lake profiles ranges from 0.4% to 3.6% and 0.9% to 8.9%, respectively. The average calculated loss (reported above) compared to calculations without considering retention is 0.8% and 2.0% for the Pinedale and Bull Lake profiles, respectively.

These loss-corrected calculated fluxes are then normalized for paleomagnetic field intensity variations over the Holocene and compared in order to evaluate the $F_{(^{10}Be_{met})}$ to this area. The Holocene-average loss-corrected $F_{(^{10}Be_{met})}$ from this study are 1.46 (± 0.20) x 10^6 atoms cm^{-2} y^{-1} and 1.30 (± 0.48) x 10^6 atoms cm^{-2} y^{-1} for the Pinedale and Bull Lake moraines, respectively (Table 3).

The predicted Holocene-average $F_{(^{10}Be_{met})}$ of Graly et al. (2011) for this site is 0.83 (± 0.08) x 10^6 atoms cm^{-2} y^{-1} (Table 3). As the pre-industrial flux map of Heikkilä and von Blanckenburg (2015) already presents a Holocene-average $F_{(^{10}Be_{met})}$ of 1.38 (+ 0.99) x 10^6 atoms cm^{-2} y^{-1}, no normalization for this method needs to be carried out.

5 Discussion

5.1 Cosmogenic Nuclide Profiles

An approximately exponential decrease in $^{10}Be_{met}$ with depth is observed for the Pinedale and Bull Lake moraines (Fig. 2). This trend can be explained most simply by the reactive transport of dissolved $^{10}Be_{met}$ with infiltrating water (e.g. Willenbring and von Blanckenburg, 2010), as exponential $^{10}Be_{met}$ profiles are predicted by reactive transport models (Maher and von Blanckenburg, 2016).

The maximum $^{10}Be_{met}$ concentration for the Pinedale moraine is measured at 10 cm depth, rather than the most surficial sample (3 cm). This peak concentration corresponds with the clay rich layer of the B-horizon in the soil profile (Table 2). This potentially indicates that this layer acts as a zone of illuviation, often observed in soil profiles that contain a mid-depth

Deleted: and
Deleted: Monte Carlo simulation
Deleted: 4.9% and 0.8% to 15.4%,
Deleted: 52 (+
Deleted: 11/-0.21
Deleted: 31 (+
Deleted: 43/-0.50
Deleted: 1

clay-rich horizon (e.g. Monaghan et al., 1992) formed by vertical transport of soil particles containing $^{10}Be_{met}$ (Jagercikova et al., 2016). This subsurface maximum could be the result of smaller grain sizes within this horizon, as these grains have a higher surface area per unit mass and can exchange ions more easily (Brown et al., 1992; Willenbring and von Blanckenburg, 2010). Alternatively, enhanced $^{10}Be_{met}$ incorporation into the lattices of newly formed clays and oxyhydroxides at depth (e.g. Barg et al., 1997) might explain this maximum. This phenomenon is not observed for the Bull Lake moraine; the highest clay content observed in the profile is in the Bk-horizon at a depth of 43 cm (Schaller et al., 2009a,b), however no increase or anomalous high $^{10}Be_{met}$ concentration is observed (Fig. 2, Table 2). It is possible that such an increase may have been missed in the Bull Lake profile, as the equivalent 10 cm depth interval was not sampled.

Deleted: 1).

Peculiarly, the observed mixing depths for the Pinedale and Bull Lake moraines as determined from the $^{10}Be_{in\ situ}$ depth profiles of Schaller et al. (2009a) (~40 and 50 cm, respectively) are not observed for the $^{10}Be_{met}$ depth profiles (Fig. 2). A couple of viable reasons for a lack of a mixing signal in the $^{10}Be_{met}$ depth profiles exist. The different grain sizes analyzed here and in Schaller et al. (2009a) might exhibit different diffusion coefficients, by which larger grain sizes are more easily mixed, however a trend in smaller grain size fractions with depth within the $^{10}Be_{in\ situ}$ mixing layer would likely be observed if this were the case. Unfortunately, separate grain size classes were not measured for $^{10}Be_{in\ situ}$ within the full mixing zone of either profile to further assess this explanation. Another possibility is that the advection of $^{10}Be_{met}$ from the surface swamps the effect of mixing that is apparent in the $^{10}Be_{in\ situ}$ depth profiles. This could indicate that continual $^{10}Be_{met}$ delivery and reactive flow resets the $^{10}Be_{met}$ profile at timescales much shorter than that of physical mixing. Profiles with a relatively low surficial pH (<5) might be particularly susceptible to this phenomenon due to incomplete retention or differential mobility of $^{10}Be_{met}$ (Kaste and Baskaran, 2011), although the profiles analyzed here are not likely to show appreciable (>9%) $^{10}Be_{met}$ loss at depth due to retention issues. Nonetheless, the formation of a clay horizon in the Pinedale moraine may indicate that soil horizonation happens more rapidly than soil mixing, as inferred from the $^{10}Be_{in\ situ}$ depth profile (Schaller et al., 2009a), suggesting that $^{10}Be_{met}$ advection from the surface is a more likely explanation.

Deleted: an observable

Deleted: 15

5.1.1 $^{10}Be_{met}$ Retention

A range of possibilities exist for retention effects and associated surficial $^{10}Be_{met}$ loss for these profiles. For the highest K_d estimate, at 1 x 10^6 L kg^{-1}, potential loss is as low as 0.4% and 0.8% for the Pinedale and Bull Lake profiles, respectively. For an average K_d of 5.5 x 10^5 L kg^{-1}, the potential loss is likewise negligible, at 0.8% and 2.0% for the Pinedale and Bull Lake profiles, respectively. On the other hand, for the lowest K_d estimate, at 1 x 10^5 L kg^{-1}, $^{10}Be_{met}$ loss due to desorption could be as great as 3.6% and 8.9% at the surface of the Pinedale and Bull Lake profiles, respectively. While the possibility of desorption cannot be ruled out, it's unlikely that either profile has experienced loss to such a degree, as pH, and thus K_d and retentivity, increases with depth. Even in the worst-case scenario of assuming maximum possible loss at the lowest K_d estimate, the magnitude of the potential loss does not substantially affect our calculated $F_{(^{10}Be_{met})}$ estimates within uncertainties. Our calculations thus capture the potential maximum bound for loss via propagated uncertainties.

5.2 $^{10}Be_{met}$ flux estimation; sources of variability

The calculated, loss- and paleointensity-corrected $F_{(^{10}Be_{met})}$ of 1.46 (± 0.20) x 10^6 atoms cm^{-2} y^{-1} and 1.30 (± 0.48) x 10^6 atoms cm^{-2} y^{-1} for the Pinedale and Bull Lake moraines, respectively, are higher compared to that estimated by Graly et al. (2011), at 0.83 x 10^6 atoms cm^{-2} y^{-1}, and agree within uncertainty with that predicted by Heikkilä and von Blanckenburg (2015), at 1.38 x 10^6 atoms cm^{-2} y^{-1} (Table 3). The considerable discrepancy between the predicted $F_{(^{10}Be_{met})}$ of each method arises primarily from differences in how each methodology treats the influence that precipitation rate has on the flux to a given area and, in particular for this study, how large of an area is covered. The 310 km x 228 km flux map grid cell of Heikkilä and von Blanckenburg (2015) covers the entirety of the Wind River Range and the surrounding, relatively low-lying flatlands (Fig. 1), where precipitation estimates vary considerably, by over an order of magnitude (WRCC, 2005), due to elevation and topographic effects on precipitation (Hostetler and Clark, 1997). For example, if one were to estimate $F_{(^{10}Be_{met})}$ from Graly et al. (2011) via (Eq. 1) to nearby Fish Lake Mountain contained within the same Heikkilä and von Blanckenburg (2015) grid cell as this study site, with a modern precipitation rate of 128 cm y^{-1} (WRCC, 2005), the $F_{(^{10}Be_{met})}$ would be 2.5 x 10^6 atoms cm^{-2} y^{-1}, substantially higher than that predicted from Heikkilä and von Blanckenburg (2015).

Deleted: 4.9

Deleted: 15.4

Deleted: Despite this, the Monte Carlo simulations indicate a low probability for loss to this degree, particularly for the Pinedale profile, as evidenced by the relatively shallow tail for each histogram (Fig. S1), with $F_{(^{10}Be_{met})}$ results within the 95% confidence interval. …

Deleted: we note

Deleted: $^{10}Be_{met}$ mobilization to

Deleted: does not have an appreciable effect on $F_{(^{10}Be_{met})}$ in the vast majority of simulations.

Deleted: 52 (+

Deleted: 11/-0.21

Deleted: 31 (+

Deleted: 43/-0.50

Considering this alone, it is not surprising that such a discrepancy exists between methods, nor is this a unique occurrence (e.g. Jungers et al., 2009; Schoonejans et al., 2017; Dixon et al., 2018; Deng et al., 2020).

Each approach has its own set of shortcomings, precluding agreement between each approach in sites such as this. The flux map of Heikkilä and von Blanckenburg (2015) has a coarse resolution and does not handle short wavelength orographic effects well, along with being model based and requiring many assumptions on atmospheric scavenging. The formula of Graly et al. (2011), on the other hand, does not take atmospheric circulation into account, instead relying on data from sites with relatively high rates of precipitation to derive an empirical formula. Recent work by Deng et al. (2020) highlights the potential for precipitation estimates to differ from GCM-derived estimates due to short timescale additive effects (*sensu* Willenbring and von Blanckenburg, 2010). Further, they find that in the majority of studies globally, GCM- and soil-derived $F_{(^{10}Be_{met})}$ estimates agree within a factor of two. That the calculated fluxes of this study agree with the GCM-modelled pre-industrial $F_{(^{10}Be_{met})}$ of Heikkilä and von Blanckenburg (2015) provides further evidence of this general observation. In any event, the strength of future $^{10}Be_{met}$ studies relies upon careful consideration of beryllium retention, spatial scale, and paleomagnetic intensity when determining $F_{(^{10}Be_{met})}$. As calculating a long-term delivery rate of $F_{(^{10}Be_{met})}$ for a particular site using $^{10}Be_{in\ situ}$ and $^{10}Be_{met}$ is both costly and time-intensive, it is especially prudent to estimate $F_{(^{10}Be_{met})}$ using both methods compared here for robust calculations utilizing $F_{(^{10}Be_{met})}$ (e.g. $^{10}Be_{met}$-derived erosion rates) in the future.

Deleted: .

Deleted: rate calculations

6. Conclusions

In this study, we compare new meteoric ^{10}Be ($^{10}Be_{met}$) and previously published *in situ*-produced ^{10}Be ($^{10}Be_{in\ situ}$) depth profile measurements from the well-characterized Pinedale (~21-25 ky) and Bull Lake (~140 ky) moraines of Wind River, Wyoming. Our ability to utilize previous knowledge of transient erosion rates from the $^{10}Be_{in\ situ}$ depth profile measurements of Schaller et al. (2009a), recalculated with revised parameters, allows us to calculate loss-corrected Holocene average $^{10}Be_{met}$ fluxes of 1.46 (± 0.20) x 10^6 atoms cm^{-2} y^{-1} and 1.30 (± 0.48) x 10^6 atoms cm^{-2} y^{-1} to the Pinedale and Bull Lake moraines, respectively. Comparing these fluxes to two independent estimation methods reveals that the empirical flux

Deleted: 52 (+

Deleted: 11/-0.21

Deleted: 31 (+

Deleted: 43/-0.50

Deleted: widely-used

estimate of Graly et al. (2011), after normalizing for Holocene paleomagnetic intensity, at 0.83 (± 0.08) x 10^6 atoms cm^{-2} y^{-1}, is lower than the calculated fluxes, and the modeled Holocene flux estimate of Heikkila and von Blanckenburg (2015), at 1.38 x 10^6 atoms cm^{-2} y^{-1}, agrees within uncertainty to the calculated fluxes. We find that loss of $^{10}Be_{met}$ in these profiles due to pH-influenced mobility/dissolution effects exerts a relatively minor potential control (biasing from <1% up to 9% in the most extreme case) on flux calculations. Inspection of the $^{10}Be_{met}$ depth profiles and their near-surface concentrations suggest that soil mixing to depths of 40 and 50 cm, as observed for the Pinedale and Bull Lake $^{10}Be_{in\ situ}$ depth profiles, respectively, is not represented by the finer grain sizes analyzed in this study. The lack of a mixing signal may be most simply explained by a swamping effect from continual delivery and advection of $^{10}Be_{met}$ from the surface that occurs over more rapid timescales than soil mixing. These differences in the depth-concentration relationships between $^{10}Be_{met}$ and $^{10}Be_{in\ situ}$ might open up a new area of research to study particle movement in soils.

Deleted: 15%)

Author Contribution

TC is a current Ph.D. student at Stanford University and conducted the majority of the work during 2018-2019 under the supervision of JWK, who contributed to several drafts of the original manuscript as well as preparation of the meteoric data set at GFZ Potsdam. MS and JDB contributed via ^{10}Be data acquisition, interpretation, and discussion; MC and PWK contributed via AMS measurements at ETH-Zurich. FvB assisted in interpretation of the comparative data set and associated discussion of meteoric ^{10}Be flux estimates, mobility/retention, and paleomagnetic field intensity normalization and contributed to manuscript drafts.

Deleted: .

Competing Interests

The authors declare no competing interests for this manuscript.

Acknowledgement

This work was made possible through the German Science Foundation Grant *BL562/7* and an Alexander von Humboldt Postdoctoral Fellowship. Support for TC came from a Career grant to Willenbring from NSF #1651243. The authors thank three anonymous reviewers for constructive comments and suggestions which greatly improved the manuscript.

References

Bacon, A. R., Richter, D. D., Bierman, P. R., and Rood, D. H.: Coupling meteoric 10Be with pedogenic losses of 9Be to improve soil residence time estimates on an ancient North American interfluve, Geology, 40(9), 847-850, https://doi.org/10.1130/G33449.1, 2012

Barg, E., Lal, D., Pavich, M. J., Caffee, M. W., and Southon, J. R.: Beryllium geochemistry in soils; evaluation of 10Be/ 9Be ratios in authigenic minerals as a basis for age models. Chemical Geology, 140, 237-258, https://doi.org/10.1016/S0009-2541(97)00051-X, 1997.

Blum, J. D., and Erel, Y.: Rb/Sr isotope systematics of a granitic soil chronosequence: The importance of biotite weathering, Geochimica et Cosmochimica Acta, 61(15), 3193-3204, https://doi.org/10.1016/S0016-7037(97)00148-8, 1997.

Borchers, B., Marrero, S., Balco, G., Caffee, M., Goehring, B., Lifton, N., ... and Stone, J.: Geological calibration of spallation production rates in the CRONUS-Earth project, Quaternary Geochronology, 31, 188-198, https://doi.org/10.1016/j.quageo.2015.01.009, 2016.

Bourlès, D.: Étude de la géochimie de l'isotope cosmogénique ^{10}Be et de son isotope stable 9Be en milieu océanique: application à la datation des sédiments marins, Ph.D. thesis, Université Paris XI, Centre d'Orsay, 1988.

Boschi, V., Willenbring, J.K.:The role of pH, organic matter composition and mineralogy on the sorption behavior of beryllium. Environmental Chemistry. http://dx.doi.org/10.1071/EN15107, 2016a.

Boschi, V., Willenbring, J.K.: Beryllium Desorption from Minerals and Organic Ligands Over Time. Chemical Geology, 439(7) 52–58. http://dx.doi.org/10.1016/j.chemgeo.2016.06.009, 2016b.

Brown, L.: 10Be as a tracer of erosion and sediment transport. Chemical Geology: Isotope Geoscience section, 65(3-4), 189-196, https://doi.org/10.1016/0168-9622(87)90002-9, 1987.

Brown, L., Pavich, M. J., Hickman, R. E., Klein, J., Middleton, R.: Erosion of the Eastern United States observed with 10Be. Earth Surface Processes and Landforms, 13, 441-457, https://doi.org/10.1002/esp.3290130509, 1988.

Brown, E. T., Edmond, J. M., Raisbeck, G. M., Bourlès, D. L., Yiou, F., and Measures, C. I.: Beryllium isotope geochemistry in tropical river basins, Geochimica et Cosmochimica Acta, 56(4), 1607-1624, https://doi.org/10.1016/0016-7037(92)90228-B, 1992.

Chadwick, O. A., & Chorover, J., The chemistry of pedogenic thresholds, Geoderma, 100(3-4), 321-353, https://doi.org/10.1016/S0016-7061(01)00027-1, 2001.

Chmeleff, J., von Blanckenburg, F., Kosser, K., and Jakob, D.: Determination of the 10Be half-life by multicollecter ICP-MS and liquid scintillation counting, Nuclear Instruments and Methods in Physics Research Section B: Beam Interactions with Materials and Atoms, 268(2), 192–199, https://doi.org/10.1016/j.nimb.2009.09.012, 2010.

Christl, M., Lippold, J., Steinhilber, F., Bernsdorff, F., and Mangini, A.: Reconstruction of global 10Be production over the past 250 ka from highly accumulating Atlantic drift sediments, Quaternary Science Reviews, 29(19-20), 2663-2672, https://doi.org/10.1016/j.quascirev.2010.06.017, 2010.

Deng, K., Wittmann, H., and von Blanckenburg, F.: The depositional flux of meteoric cosmogenic 10Be from modelling and observation, Earth and Planetary Science Letters, 550, 116530, https://doi.org/10.1016/j.epsl.2020.116530, 2020.

Dixon, J. L., Chadwick, O. A., and Pavich, M. J.: Climatically controlled delivery and retention of meteoric 10Be in soils, Geology, 46(10), 899-902, https://doi.org/10.1130/G45176.1, 2018.

Dunai, T. J.: Scaling factors for production rates of in situ produced cosmogenic nuclides: a critical reevaluation, Earth and Planetary Science Letters, 176(1), 157-169, https://doi.org/10.1016/S0012-821X(99)00310-6, 2000.

Easterbrook, D. J., Pierce, K., Gosse, J., Gillespie, A., Evenson, E., and Hamblin, K.: Quaternary geology of the western United States, in: Quaternary Geology of the United States, edited by: Easterbrook, D. J., Desert Res. Inst., Reno, Nev., 19-79, 2003.

Ebert, K., Willenbring, J., Norton, K. P., Hall, A., and Hättestrand, C.: Meteoric 10Be concentrations from saprolite and till in northern Sweden: Implications for glacial erosion and age, Quaternary Geochronology, 12, 11-22, https://doi.org/10.1016/j.quageo.2012.05.005, 2012.

Field, C. V., Schmidt, G. A., Koch, D., and Salyk, C.: Modeling production and climate-related impacts on 10Be concentration in ice cores, Journal of Geophysical Research: Atmospheres, 111(D15), https://doi.org/10.1029/2005JD006410, 2006.

Frank, M., Schwarz, B., Baumann, S., Kubik, P. W., Suter, M., and Mangini, A.: A 200 kyr record of cosmogenic radionuclide production rate and geomagnetic field intensity from 10Be in globally stacked deep-sea sediments, Earth and Planetary Science Letters, 149(1-4), 121-129, https://doi.org/10.1016/S0012-821X(97)00070-8, 1997.

Guelke-Stelling, M., and von Blanckenburg, F.: Fe isotope fractionation caused by translocation of iron during growth of bean and oat as models of strategy I and II plants, Plant and soil, 352(1-2), 217-231, https://doi.org/10.1007/s11104-011-0990-9, 2012.

Gosse, J. C., Klein, J., Lawn, B., Middleton, R., and Evenson, E. B.: Beryllium-10 dating of the duration and retreat of the last Pinedale glacial sequence, Science, 268(5215), 1329-1333, https://doi.org/10.1126/science.268.5215.1329, 1995.

Graly, J. A., Bierman, P. R., Reusser, L. J., and Pavich, M. J.: Meteoric ^{10}Be in soil profiles—a global meta-analysis, Geochimica et Cosmochimica Acta, 74(23), 6814-6892, https://doi.org/10.1016/j.gca.2010.08.036, 2010.

Graly, J. A., Reusser, L. J., and Bierman, P. R.: Short and long-term delivery rates of meteoric 10Be to terrestrial soils, Earth and Planetary Science Letters, 302(3-4), 329-336, https://doi.org/10.1016/j.epsl.2010.12.020, 2011.

Hall, R. D., and Shroba, R. R.: Soil evidence for a glaciation intermediate between the Bull Lake and Pinedale glaciations at Fremont Lake, Wind River Range, Wyoming, USA, Arctic and Alpine Research, 27(1), 89-98, https://doi.org/10.2307/1552071, 1995.

Heikkilä, U. and Smith, A. M.: Influence of model resolution on the atmospheric transport of 10Be, Atmospheric Chemistry and Physics, 12(21), 10601-10612, https://doi.org/10.5194/acp-12-10601-2012, 2012.

Heikkilä, U. and Von Blanckenburg, F.: The global distribution of Holocene meteoric 10Be fluxes from atmospheric models, GFZ Data Services, GFZ Potsdam, Germany, http://doi.org/10.5880/GFZ.3.4.2015.001, 2015.

Hostetler, S. W., and Clark, P. U.: Climatic controls of western US glaciers at the last glacial maximum, Quaternary Science Reviews, 16(6), 505-511, https://doi.org/10.1016/S0277-3791(96)00116-3, 1997.

Jagercikova, M., Cornu, S., Bourlès, D., Evrard, O., Hatté, C. and Balesdent, J.: Quantification of vertical solid matter transfers in soils during pedogenesis by a multi-tracer approach, Journal of Soils and Sediments, 17, 408-422, https://doi.org/10.1007/s11368-016-1560-9, 2016.

Jelinski, N., Willenbring, J.K., Schumacher, T.E., Li, S. Lobb, D.A., Papiernik, S.K., and Yoo, K.: Meteoric Beryllium-10 as a tracer of cumulative erosion due to post-settlement land use in west-central Minnesota, USA, Journal of Geophysical Research – Earth Surface, 124(4), 874-901, https://doi.org/10.1029/2018JF004720, 2019.

Jungers, M. C., Bierman, P. R., Matmon, A., Nichols, K., Larsen, J., and Finkel, R.: Tracing hillslope sediment production and transport with in situ and meteoric 10Be, Journal of Geophysical Research: Earth Surface, 114(F4), https://doi.org/10.1029/2008JF001086, 2009.

Kaste, J. M., and Baskaran, M.: Meteoric 7Be and 10Be as process tracers in the environment, in: Handbook of environmental isotope geochemistry, edited by: Baskaran, M., Springer, Berlin, Heidelberg, 61-85, https://doi.org/10.1007/978-3-642-10637-8_5, 2012.

Kubik, P. W., and Christl, M.: 10Be and 26Al measurements at the Zurich 6 MV Tandem AMS facility, Nuclear Instruments and Methods in Physics Research Section B: Beam Interactions with Materials and Atoms, 268(7-8), 880-883, https://doi.org/10.1016/j.nimb.2009.10.054, 2010.

Kohl, C. P., and Nishiizumi, K.: Chemical isolation of quartz for measurement of in-situ -produced cosmogenic nuclides, Geochimica et Cosmochimica Acta, 56(9), 3583-3587, https://doi.org/10.1016/0016-7037(92)90401-4, 1992.

Lal, D. and Peters, B.: Cosmic ray produced radioactivity on the Earth, in: Kosmische Strahlung II/Cosmic Rays II, edited by: Sitte, K., Springer, Berlin, Heidelberg, 551-612, https://doi.org/10.1007/978-3-642-46079-1_7, 1967.

Mahaney, W. C., and Halvorson, D. L.: Rates of mineral weathering in the Wind River Mountains, western Wyoming, in: Rates of chemical weathering of rocks and minerals, edited by: Colman, S., and Dethier, D., Academic Press, Cambridge, Massachusetts, 147-167, 1986.

Maher, K., and von Blanckenburg, F.: Surface ages and weathering rates from 10Be (meteoric) and 10Be/9 Be: insights from differential mass balance and reactive transport modeling, Chemical Geology, 446, 70-86, https://doi.org/10.1016/j.chemgeo.2016.07.016, 2016.

Masarik, J., and Beer, J.: Simulation of particle fluxes and cosmogenic nuclide production in the Earth's atmosphere, Journal of Geophysical Research: Atmospheres, 104(D10), 12099-12111, https://doi.org/10.1029/1998JD200091, 1999.

Masarik, J., and Beer, J.: An updated simulation of particle fluxes and cosmogenic nuclide production in the Earth's atmosphere, Journal of Geophysical Research: Atmospheres, 114(D11), https://doi.org/10.1029/2008JD010557, 2009.

Mckean, J.A., Dietrich, W.E., Finkel, R.C., Southon, J.R., and Caffee, M.W.: Quantification of Soil Production and Downslope Creep Rates from Cosmogenic Be-10 Accumulations on a Hillslope Profile, Geology, 21, 343-346, https://doi.org/10.1130/0091-7613(1993)021<0343:QOSPAD>2.3.CO;2, 1993.

Monaghan, M. C., McKean, J., Dietrich, W., and Klein, J.: 10Be chronometry of bedrock-to-soil conversion rates, Earth and Planetary Science Letters, 111(2-4), 483-492, https://doi.org/10.1016/0012-821X(92)90198-5, 1992.

Ouimet, W., Dethier, D., Bierman, P., Wyshnytzkyr, C., Shea, N., and Rood, D. H.: Spatial and temporal variations in meteoric 10Be inventories and long-term deposition rates, Colorado Front Range, Quaternary Science Reviews, 109, 1-12, https://doi.org/10.1016/j.catena.2014.12.008, 2015.

Pavich, M. J., Brown, L., Harden, J., Klein, J., and Middleton, R.: 10Be distribution in soils from Merced River terraces, California, Geochimica et Cosmochimica Acta, 50(8), 1727-1735, https://doi.org/10.1016/0016-7037(86)90134-1, 1986.

Phillips, F. M., Zreda, M. G., Gosse, J. C., Klein, J., Evenson, E. B., Hall, R. D., Chadwick, O.A., and Sharma, P.: Cosmogenic 36Cl and 10Be ages of Quaternary glacial and fluvial deposits of the Wind River Range, Wyoming, Geological Society of America Bulletin, 109(11), 1453-1463, https://doi.org/10.1130/0016-7606(1997)109<1453:CCABAO>2.3.CO;2, 1997.

Phillips, F. M., Argento, D. C., Balco, G., Caffee, M. W., Clem, J., Dunai, T. J., ... and Jull, A. T.: The CRONUS-Earth project: a synthesis, Quaternary Geochronology, 31, 119-154, https://doi.org/10.1016/j.quageo.2015.09.006, 2016.

Pigati, J. S. and Lifton, N. A.: Geomagnetic effects on time-integrated cosmogenic nuclide production with emphasis on in situ 14C and 10Be, Earth and Planetary Science Letters, 226(1-2), 193-205, https://doi.org/10.1016/j.epsl.2004.07.031, 2004.

Portenga, E.W., Bierman, P.R., Trodick Jr, C.D., Greene, S.E., DeJong, B.D., Rood, D.H., and Pavich, M.J.: Erosion rates and sediment flux within the Potomac River basin quantified over millennial timescales using beryllium isotopes, GSA Bulletin, 131(7-8), 1295-1311, https://doi.org/10.1130/B31840.1, 2019.

Reusser, L., Graly, J., Bierman, P., and Rood, D.: Calibrating a long-term meteoric 10Be accumulation rate in soil, Geophysical Research Letters, 37(19), https://doi.org/10.1029/2010GL044751, 2010.

Richmond, G. M.: Geologic map of the Fremont Lake south quadrangle, Sublette County, Wyoming, Map 1138, https://doi.org/10.3133/gq1138, 1973.

Schaller, M., Ehlers, T. A., Blum, J. D., and Kyrllenberg, M. A.: Quantifying glacial moraine age, denudation, and soil mixing with cosmogenic nuclide depth profiles, Journal of Geophysical Research: Earth Surface, 114(F1), https://doi.org/10.1029/2007JF000921, 2009a.

Schaller, M., Blum, J. D., & Ehlers, T. A.: Combining cosmogenic nuclides and major elements from moraine soil profiles to improve weathering rate estimates, Geomorphology, 106(3-4), 198-205, https://doi.org/10.1016/j.geomorph.2008.10.014, 2009b.

Schoonejans, J., Vanacker, V., Opfergelt, S., and Christl, M.: Long-term soil erosion derived from in-situ 10Be and inventories of meteoric 10Be in deeply weathered soils in southern Brazil. Chemical Geology, 466, 380-388, https://doi.org/10.1016/j.chemgeo.2017.06.025, 2017.

Sharp, W. D., Ludwig, K. R., Chadwick, O. A., Amundson, R., and Glaser, L. L.: Dating fluvial terraces by 230 Th/U on pedogenic carbonate, Wind River Basin, Wyoming, Quaternary Research, 59(2), 139-150, https://doi.org/10.1016/S0033-5894(03)00003-6, 2003.

Steinhilber, F., Abreu, J. A., Beer, J., and McCracken, K. G.: Interplanetary magnetic field during the past 9300 years inferred from cosmogenic radionuclides, Journal of Geophysical Research: Space Physics, 115(A1), https://doi.org/10.1029/2009JA014193, 2010.

Stone, J. O.: Air pressure and cosmogenic isotope production, Journal of Geophysical Research: Solid Earth, 105(B10), 23753-23759, https://doi.org/10.1029/2000JB900181, 2000.

Taylor, A. and Blum, J. D.: Relation between soil age and silicate weathering rates determined from the chemical evolution of a glacial chronosequence, Geology, 23(11), 979-982, https://doi.org/10.1130/0091-7613(1995)023<0979:RBSAAS>2.3.CO;2, 1995.

Taylor, A. and Blum, J. D.: Relation between soil age and silicate weathering rates determined from the chemical evolution of a glacial chronosequence: Reply, Geology, 25(4), 382-383, 1997.

Valet, J. P., Meynadier, L., and Guyodo, Y.: Geomagnetic dipole strength and reversal rate over the past two million years, Nature, 435(7043), 802-805, https://doi.org/10.1038/nature03674, 2005.

von Blanckenburg, F., Hewawasam, T., and Kubik, P. W.: Cosmogenic nuclide evidence for low weathering and denudation in the wet, tropical highlands of Sri Lanka, Journal of Geophysical Research: Earth Surface, 109(F3), https://doi.org/10.1029/2003JF000049, 2004.

von Blanckenburg, F., Bouchez, J., and Wittmann, H.: Earth surface erosion and weathering from the 10Be (meteoric)/9Be ratio, Earth and Planetary Science Letters, 351, 295-305, https://doi.org/10.1016/j.epsl.2012.07.022, 2012.

von Blanckenburg, F., and Bouchez, J.: River fluxes to the sea from the ocean's 10Be/9Be ratio. Earth and Planetary Science Letters, 387, 34-43, https://doi.org/10.1016/j.epsl.2013.11.004, 2014.

von Blanckenburg, F., Bouchez, J., Ibarra, D.E., and Maher, K.: Stable runoff and weathering fluxes into the oceans over Quaternary climate cycles, Nature Geoscience, 8, 538-U146, https://doi.org/10.1038/ngeo2452, 2015.

Willenbring, J. K., and von Blanckenburg, F.: Meteoric cosmogenic Beryllium-10 adsorbed to river sediment and soil: Applications for Earth-surface dynamics. Earth-Science Reviews, 98(1-2), 105-122, https://doi.org/10.1016/j.earscirev.2009.10.008, 2010.

Wittmann, H., Von Blanckenburg, F., Bouchez, J., Dannhaus, N., Naumann, R., Christl, M., and Gaillardet, J.: The dependence of meteoric 10Be concentrations on particle size in Amazon River bed sediment and the extraction of reactive 10Be/9Be ratios, Chemical Geology, 318, 126-138, https://doi.org/10.1016/j.chemgeo.2012.04.031, 2012.

Western Regional Climate Center (WRCC): https://wrcc.dri.edu/, last access: 18 September 2020, 2005.

You, C. F., Lee, T., and Li, Y. H.: The partition of Be between soil and water. Chemical Geology, 77(2), 105-118, https://doi.org/10.1016/0009-2541(89)90136-8, 1989.

Figures

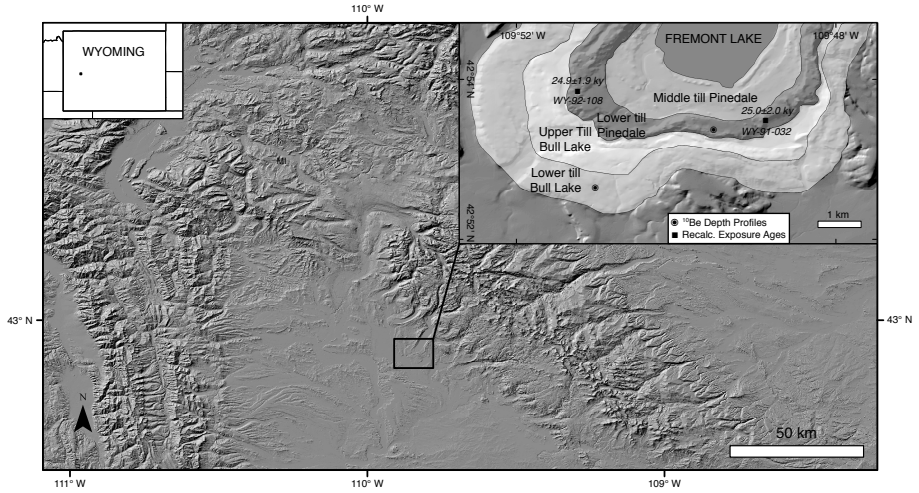

760 **Fig. 1)** Hillshade map of the Wind River range, derived from a 10 m digital elevation model (DEM); regional map encompasses the entirety of the meteoric ^{10}Be flux map grid cell of Heikkila and von Blanckenburg (2015). Inset (upper left) shows location of regional map within Wyoming. Inset (upper right) shows locations of depth profiles analyzed for cosmogenic nuclide concentrations from the terminal Pinedale and Bull Lake moraines in the Fremont Lake area (after Richmond [1973] and Schaller et al. [2009a]). Also shown are the locations of boulder surface exposure dates for the
765 Pinedale moraine (WY-92-108 and WY-91-032 of Gosse et al., 1995) that were recalculated using revised parameters (Table S1) to establish an updated independent age constraint for this moraine.

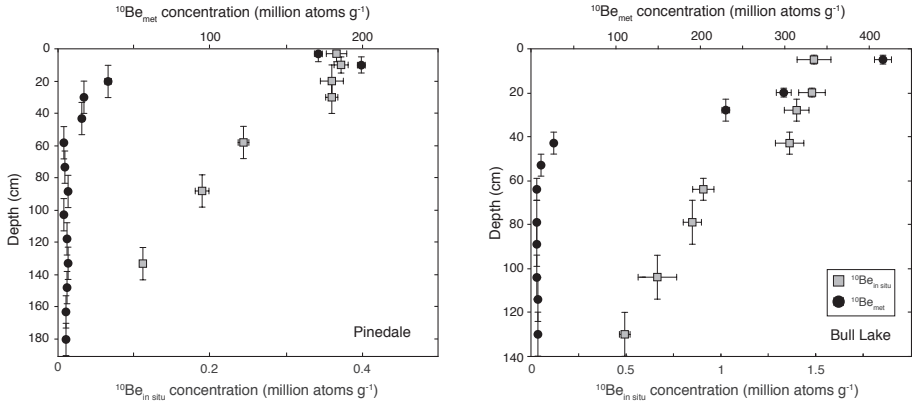

Fig. 2) (Left) Depth profile for the Pinedale moraine; $^{10}Be_{met}$ concentrations were measured from the <2 mm grain-size fraction of 14 samples from the same depth profile as analyzed for $^{10}Be_{in\ situ}$ in Schaller et al. (2009a). (Right) Depth profile for the Bull Lake moraine; $^{10}Be_{met}$ concentrations were also measured from the <2 mm grain-size fraction of 11 samples from the same depth profile as analyzed for $^{10}Be_{in\ situ}$ in Schaller et al. (2009a). The $^{10}Be_{met}$ concentration at 94 cm was not measured.

Table 1. Recalculated Chi-Square Solutions for Different Denudation Rate Simulations of Schaller et al. (2009a)[a]

Type of Denudation	Model	Age (ky; *fixed parameter*)	Average Denudation (mm ky^{-1})	Inherited ^{10}Be concentration (10^5 at g^{-1})	Mixing Depth (cm)	Diffusivity *k* (10^{-3} m^2 y^{-1})	Maximum Height (m)	Slope Angle (degrees)
		Pinedale moraine (2262 m asl, 42° 53′ 26″ N, 109° 49′ 34″ W)						
Constant	2	25	15	0.2	0			
Transient	4	25	29-35	0.2	0	20	30	25,30
		Bull Lake moraine (2285 m asl, 42° 52′ 39″ N, 109° 51′ 00″ W)						
Constant	6	140	7.5	1.4	0			
Transient	8	140	6-21	1.2-1.8	0	0.3-10	35,40,50,60	5,10,15, 20,25,30

[a]For a full explanation of range allowed and resolution of each parameter, see Table 3 of *Schaller et al. (2009a)*

Table 1. ^{10}Be Concentrations and GSD[a] in Depth Profiles from Pinedale and Bull Lake Moraines

Sample[b]	Depth (cm)	Sand (wt %)	Silt (wt%)	Clay (wt %)	*In situ* ^{10}Be concentration[c] (10^5 atoms g^{-1})	Meteoric ^{10}Be sample weight (g)	^{9}Be carrier weight (mg)	Meteoric ^{10}Be concentration[c] (10^6 atoms g^{-1})	Meteoric ^{10}Be inventory[d] (10^6 atoms cm^{-2})
Pinedale moraine (2262 m asl, 42° 53′ 26″ N, 109° 49′ 34″ W)									
04-WRMP-014	3 ± 2	75	18	6	3.67 ± 0.14	4.5747	0.2146	171.283 ± 5.142	1006 ± 30
04-WRMP-013	10 ± 5	68	22	10	3.73 ± 0.09	3.1697	0.2146	199.526 ± 5.986	2743 ± 84
04-WRMP-012	20 ± 10	70	23	7	3.60 ± 0.15	6.4287	0.2146	33.007 ± 3.183	588 ± 64
04-WRMP-011	30 ± 10	74	22	4	3.60 ± 0.08	6.1094	0.2148	16.819 ± 1.541	265 ± 31
04-WRMP-010	43 ± 10	76	19	5	-	5.1606	0.2144	15.357 ± 1.189	306 ± 31
04-WRMP-009	58 ± 10	82	15	3	2.44 ± 0.07	5.6470	0.2146	3.966 ± 0.336	11 ± 10
04-WRMP-008	73 ± 10	85	12	3	-	5.4438	0.2142	4.673 ± 0.382	33 ± 11
04-WRMP-007	88 ± 10	81	16	3	1.89 ± 0.09	5.6027	0.2140	6.699 ± 0.563	94 ± 17
04-WRMP-006	103 ± 10	82	15	3	-	6.0067	0.2103	3.569 ± 0.322	0 ± 10
04-WRMP-005	118 ± 10	71	23	6	-	3.0500	0.2127	6.207 ± 0.284	79 ± 9
04-WRMP-004	133 ± 10	71	24	5	1.11 ± 0.03	3.1070	0.2134	6.489 ± 0.302	88 ± 9
04-WRMP-003	148 ± 10	74	21	6	-	2.9340	0.2128	5.656 ± 0.249	63 ± 7
04-WRMP-002	163 ± 10	72	22	6	-	2.8869	0.2107	5.531 ± 0.240	59 ± 7
04-WRMP-001	180 ± 10	72	23	6	-	3.0824	0.2135	5.098 ± 0.236	52 ± 8
								∫	5387 ± 122
Bull Lake moraine (2285 m asl, 42° 52′ 39″ N, 109° 51′ 00″ W)									
AT-FL-4L	5 ± 2	69	22	9	14.9 ± 0.9	1.0174	0.4125	415.475 ± 12.464	4092 ± 125
AT-FL-4K	20 ± 5	51	29	20	14.8 ± 0.7	1.0793	0.2139	298.813 ± 8.965	8774 ± 269
AT-FL-4J	28 ± 5	52	34	14	14.0 ± 0.6	1.0824	0.2140	230.442 ± 6.913	3585 ± 111
AT-FL-4I	43 ± 5	47	23	30	12.3[α] ± 0.7	1.0593	0.1963	26.590 ± 0.798	608 ± 24
AT-FL-4H	53 ± 5	50	28	22	-	1.0176	0.2141	11.433 ± 0.343	102 ± 7
AT-FL-4G	64 ± 5	54	26	20	9.08 ± 0.56	1.0109	0.2144	7.083 ± 0.382	17 ± 8
AT-FL-4F	79 ± 10	60	24	16	8.50 ± 0.48	1.01	0.2141	6.639 ± 0.236	10 ± 7
AT-FL-4E	89 ± 10	62	24	14	-	1.0722	0.2142	6.318 ± 0.246	0 ± 5
AT-FL-4D	94 ± 10	75	17	9	-	-	-	6.723[e]	4[e]
AT-FL-4C	104 ± 10	64	26	10	5.98[α] ± 1.00	1.0164	0.2144	7.129 ± 0.428	16 ± 9
AT-FL-4B	114 ± 10	60	25	15	-	1.0283	0.2142	8.021 ± 0.241	34 ± 5
AT-FL-4A	130 ± 10	60	25	15	4.93 ± 0.28	1.0294	0.2143	8.449 ± 0.253	68 ± 8
								∫	17310 ± 318

[a]Grain size distributions and *in situ* ^{10}Be concentrations from *Schaller et al. (2009a)*

[b]See Schaller et al. (2009a) for the grain size fraction analyzed for each sample

[c]Corrected for blank, reported error includes analytical uncertainties (1σ)

[d]Corrected for inheritance

[e]Average of $^{10}Be_{met}$ concentations from directly above and below this depth

[□]Average of multiple aliquots analyzed in Schaller et al. (2009a)

Table 2. ^{10}Be Concentrations and GSD[a] in Depth Profiles from Pinedale and Bull Lake Moraines

Sample[b]	Depth (cm)	Sand (wt %)	Silt (wt%)	Clay (wt %)	*In situ* ^{10}Be concentration[c] (10^5 atoms g^{-1})	Meteoric ^{10}Be sample weight (g)	^{9}Be carrier weight (mg)	Meteoric ^{10}Be concentration[c] (10^6 atoms g^{-1})	Meteoric ^{10}Be inventory[d] (10^6 atoms cm^{-2})
Pinedale moraine (2262 m asl, 42° 53′ 26″ N, 109° 49′ 34″ W)									
04-WRMP-014	3 ± 2	75	18	6	3.67 ± 0.14	4.5747	0.2146	171.283 ± 5.142	1006 ± 30
04-WRMP-013	10 ± 5	68	22	10	3.73 ± 0.09	3.1697	0.2146	199.526 ± 5.986	2743 ± 84
04-WRMP-012	20 ± 10	70	23	7	3.60 ± 0.15	6.4287	0.2146	33.007 ± 3.183	588 ± 64
04-WRMP-011	30 ± 10	74	22	4	3.60 ± 0.08	6.1094	0.2148	16.819 ± 1.541	265 ± 31
04-WRMP-010	43 ± 10	76	19	5	-	5.1606	0.2144	15.357 ± 1.189	306 ± 31
04-WRMP-009	58 ± 10	82	15	3	2.44 ± 0.07	5.6470	0.2146	3.966 ± 0.336	11 ± 10
04-WRMP-008	73 ± 10	85	12	3	-	5.4438	0.2142	4.673 ± 0.382	33 ± 11
04-WRMP-007	88 ± 10	81	16	3	1.89 ± 0.09	5.6027	0.2140	6.699 ± 0.563	94 ± 17
04-WRMP-006	103 ± 10	82	15	3	-	6.0067	0.2103	3.569 ± 0.322	0 ± 10
04-WRMP-005	118 ± 10	71	23	6	-	3.0500	0.2127	6.207 ± 0.284	79 ± 9
04-WRMP-004	133 ± 10	71	24	5	1.11 ± 0.03	3.1070	0.2134	6.489 ± 0.302	88 ± 9
04-WRMP-003	148 ± 10	74	21	6	-	2.9340	0.2128	5.656 ± 0.249	63 ± 7
04-WRMP-002	163 ± 10	72	22	6	-	2.8869	0.2107	5.531 ± 0.240	59 ± 7
04-WRMP-001	180 ± 10	72	23	6	-	3.0824	0.2135	5.098 ± 0.236	52 ± 8
								∫	5387 ± 122
Bull Lake moraine (2285 m asl, 42° 52′ 39″ N, 109° 51′ 00″ W)									
AT-FL-4L	5 ± 2	69	22	9	14.9 ± 0.9	1.0174	0.4125	415.475 ± 12.464	4092 ± 125
AT-FL-4K	20 ± 5	51	29	20	14.8 ± 0.7	1.0793	0.2139	298.813 ± 8.965	8774 ± 269

AT-FL-4J	28 ± 5	52	34	14	14.0 ± 0.6	1.0824	0.2140	230.442 ± 6.913	3585 ± 111
AT-FL-4I	43 ± 5	47	23	30	12.3[¤] ± 0.7	1.0593	0.1963	26.590 ± 0.798	608 ± 24
AT-FL-4H	53 ± 5	50	28	22	-	1.0176	0.2141	11.433 ± 0.343	102 ± 7
AT-FL-4G	64 ± 5	54	26	20	9.08 ± 0.56	1.0109	0.2144	7.083 ± 0.382	17 ± 8
AT-FL-4F	79 ± 10	60	24	16	8.50 ± 0.48	1.01	0.2141	6.639 ± 0.236	10 ± 7
AT-FL-4E	89 ± 10	62	24	14	-	1.0722	0.2142	6.318 ± 0.246	0 ± 5
AT-FL-4D	94 ± 10	75	17	9	-	-	-	6.723[e]	4[e]
AT-FL-4C	104 ± 10	64	26	10	5.98[¤] ± 1.00	1.0164	0.2144	7.129 ± 0.428	16 ± 9
AT-FL-4B	114 ± 10	60	25	15	-	1.0283	0.2142	8.021 ± 0.241	34 ± 5
AT-FL-4A	130 ± 10	60	25	15	4.93 ± 0.28	1.0294	0.2143	8.449 ± 0.253	68 ± 8
								∫	17310 ± 318

[a]Grain size distributions and *in situ* ^{10}Be concentrations from *Schaller et al. (2009a)*

[b]See Schaller et al. (2009a) for the grain size fraction analyzed for each sample

[c]Corrected for blank, reported error includes analytical uncertainties (1σ)

[d]Corrected for inheritance

[e]Average of $^{10}Be_{met}$ concentations from directly above and below this depth

[¤]Average of multiple aliquots analyzed in Schaller et al. (2009a)

Table 3. $^{10}Be_{met}$ flux estimates, raw and normalized for Holocene paleointensity variations

Method	F($^{10}Be_{met}$) uncorrected (x 10^6 atoms $cm^{-2}y^{-1}$)	Valid over time scale (ky)	$^{10}Be_{met}$ production ratio relative to Modern	$^{10}Be_{met}$ production ratio relative to Holocene	F($^{10}Be_{met}$) corrected to represent Holocene (x 10^6 atoms $cm^{-2}y^{-1}$)
Pinedale (This Study)	1.04 (±0.14)	6	0.88[a]	0.71[a]	1.46 (±0.20)
Bull Lake (This Study)	1.04 (±0.39)	24	0.99[a]	0.80[a]	1.30 (±0.48)
Graly et al. (2011)	0.55 (± 0.05)	0.005	0.82[b]	0.67[c]	0.83 (±0.08)
Heikkilä and von Blanckenburg (2015)	-	10	1.23[c]	-	1.38 (+0.99)[d]

[a] *using measured $^{10}Be_{met}$ seafloor accumulation record of Christl et al. (2010) from*

6 ky and 24 ky to present for the Pinedale and Bull Lake moraines, respectively

[b] *using the paleomagnetic scaling method of Masarik and Beer (2009)*

[c] *using the paleomagnetic reconstruction method of Steinhilber et al. (2012)*

[d] *uncertainty represents the difference between the 'industrial' and the 'pre-industrial' modeled flux of Heikkilä and von Blanckenburg (2015)*